

Review

# Consolidation of Gold and Gadolinium Nanoparticles: An Extra Step towards Improving Cancer Imaging and Therapy

Maria Anthi Kouri <sup>1,2</sup> , Konstantina Polychronidou <sup>3</sup> , Grigorios Loukas <sup>3</sup>, Aikaterini Megapanou <sup>3</sup>, Ioanna-Aglaia Vagena <sup>3,4</sup>, Angelica M. Gerardos <sup>3,5</sup>, Ellas Spyratou <sup>1,\*</sup>  and Eftstathios P. Eftsathopoulos <sup>1,\*</sup> 

<sup>1</sup> 2nd Department of Radiology, Medical School, National and Kapodistrian University of Athens, 11527 Athens, Greece; mariakouri90@gmail.com

<sup>2</sup> Medical Physics Program, University of Massachusetts Lowell, 265 Riverside St, Lowell, MA 01854, USA

<sup>3</sup> School of Health Sciences, Medical School, National and Kapodistrian University of Athens, 75 Mikras Assias Street, 11527 Athens, Greece; konna.polychronidou@gmail.com (K.P.); amgerar@windowslive.com (A.M.G.)

<sup>4</sup> Laboratory of Biology, Department of Basic Medical Sciences, Medical School, National and Kapodistrian University of Athens, 11527 Athens, Greece

<sup>5</sup> Theoretical and Physical Chemistry Institute, National Hellenic Research Foundation, 48 Vassileos Constantinou Avenue, 11635 Athens, Greece

\* Correspondence: spyratouellas@gmail.com (E.S.); stathise@med.uoa.gr (E.P.E.)

**Abstract:** The multifactorial nature of cancer still classifies the disease as one of the leading causes of death worldwide. Modern medical sciences are following an interdisciplinary approach that has been fueled by the nanoscale revolution of the past years. The exploitation of high-Z materials, in combination with ionizing or non-ionizing radiation, promises to overcome restrictions in medical imaging and to augment the efficacy of current therapeutic modalities. Gold nanoparticles (AuNPs) have proven their value among the scientific community in various therapeutic and diagnostic techniques. However, the high level of multiparametric demands of AuNP experiments in combination with their biocompatibility and cytotoxicity levels remain crucial issues. Gadolinium NPs (GdNPs), have presented high biocompatibility, low cytotoxicity, and excellent hemocompatibility, and have been utilized in MRI-guided radiotherapy, photodynamic and photothermal therapy, etc. The utilization of gadolinium bound to AuNPs may be a promising alternative that would reduce phenomena, such as toxicity, aggregation, etc., and could create a multimodal in vivo contrast and therapeutic agent. This review highlights multi-functionalization strategies against cancer where gold and gadolinium NPs are implicated. Their experimental applications and limitations of the past 5 years will be analyzed in the hope of enlightening the benefits and drawbacks of their proper combination.

**Keywords:** gold nanoparticles; gadolinium nanoparticles; cancer imaging; cancer therapy; nanomedicine



**Citation:** Kouri, M.A.; Polychronidou, K.; Loukas, G.; Megapanou, A.; Vagena, I.-A.; Gerardos, A.M.; Spyratou, E.; Eftsathopoulos, E.P. Consolidation of Gold and Gadolinium Nanoparticles: An Extra Step towards Improving Cancer Imaging and Therapy. *J. Nanotheranostics* **2023**, *4*, 127–149. <https://doi.org/10.3390/jnt4020007>

Academic Editor: Seyed Moein Moghimi

Received: 14 March 2023

Revised: 8 April 2023

Accepted: 23 April 2023

Published: 26 April 2023



**Copyright:** © 2023 by the authors. Licensee MDPI, Basel, Switzerland. This article is an open access article distributed under the terms and conditions of the Creative Commons Attribution (CC BY) license (<https://creativecommons.org/licenses/by/4.0/>).

## 1. Introduction

Cancer is characterized by an abnormal and uncontrolled cell division coupled with malignant behavior, such as metastasis and invasion [1]. Despite remarkable advances in modern medical research, cancer's aggressive and multifactorial nature still classifies it as one of the leading causes of death worldwide. Against an opponent with so many factors, only an interdisciplinary approach could be found to be sufficient and possibly effective. The development of modern therapeutics and imaging in the field of cancer has been fueled by the nanoscale revolution of the past years. This has initiated the production of nanoparticles (NPs) to augment the efficacy of current therapeutic modalities, to overcome restrictions in medical imaging, or even to initiate multi-functionalization strategies against cancer which are even resulting in new terminologies, such as theranostics, where a nanoparticle can be simultaneously utilized in therapy and diagnosis [2].

Assuredly, one of the most common approaches is tumor radiosensitization, through the exploitation of high atomic number (Z) materials and their increased and localized

photon absorption at kVp energies. The adaptation of this approach led to experimentation with gold ( $Z = 79$ ), platinum ( $Z = 78$ ), silver ( $Z = 47$ ), and recently gadolinium ( $Z = 64$ ), etc., in combination with ionizing or non-ionizing radiation as possible therapeutic or immunogenic agents [3].

Additionally, the gold standard of cancer prevention and the ultimate achievement of oncology is early and accurate prognosis and diagnosis. Thus, there is an urgent need for new and improved functionalized contrast agents. The meticulous visualization of tumor growth and systemic monitoring of this disease could be achieved with the exploitation of high- $Z$  NPs. Their unique pharmacokinetic properties and their high levels of targeted accumulation in the body, as well as their longer vascular half-life than that of molecular contrast agents, are just a few of their beneficial properties.

Certainly, *in vivo* toxicity of nanomaterials is an adverse parameter that has to be taken into consideration. It is related not only to the NPs' elemental composition, morphology, and size, but also to their physical and chemical properties of surface ligands [4].

All of the above indicate that adequate treatment and imaging of cancer not only requires the combination of modern therapies and imaging modalities with nanomedicine but probably also requires a particular combination of nanomaterials. AuNPs have proven their value in numerous scientific initiatives throughout the last decades. Unfortunately, their clinical implementation has not yet been applied. Gd-based NPs, as high atomic number particles, have also been utilized as radiosensitizers [5–7]. Due to Gd's inherent toxicity, as part of the lanthanide group, various polymers, such as silica or polyethylenimine (PEI) pre-modified with polyethylene glycol (PEG), were used as coating on hte GdNPs' surfaces [6,8,9]. Thereinafter, GdNPs have been utilized in MRI-guided radiotherapy, photodynamic and photothermal therapy with near-infrared fluorescence imaging capabilities, and in dual mode magnetic resonance/computed tomography imaging [6,10,11]. Furthermore, they have presented high biocompatibility, low cytotoxicity, and excellent hemocompatibility [7].

Conceivably, the missing piece of the puzzle would be the consolidation of the undoubtedly beneficial AuNPs with gadolinium, which is widely employed in imaging. The utilization of gadolinium in different nanoscale sizes and shapes, bound to gold nanoparticles, may be a promising alternative that would reduce or even prevent unwanted phenomena accompanying the use of AuNPs (such as toxicity, aggregation, etc.), would enhance their stability and biocompatibility, and would successfully create a multimodal *in vivo* and real-time contrast agent.

In this review, we will attempt to collect and highlight the multi-functionalization strategies against cancer where gold and gadolinium NPs are implicated. Their most recent experimental applications and limitations will be analyzed in the hope of enlightening the benefits and drawbacks of their proper combination. In conclusion, any current applications and results of gold and gadolinium NPs' consolidation against cancer will be thoroughly presented.

## 2. Gold Nanoparticles

Among the various oxidation states of gold complexes, the most common due to their electronegativity are those of Auric (Au(I)) and Auric (Au(III)) [12,13]. In order for the aforementioned metallic states to form a stable complex in aqueous solution, they are subjugated to the complex ligand's property as well as to the donor atom of ligands attached to gold [12,14]. Research so far has indicated that stability in gold is directly proportional to the electronegativity of the donor atom. More precisely, as electronegativity increases, the stability of the gold complex drops [12,15]. This could justify why in the production of AuNPs, the two preferred precursors are gold(I) thiosulfate or gold(III) chloride complexes [12], with the latter being particularly selected as precursors.

### 2.1. Gold Nanoparticles in Medical Imaging

Since Faraday's article in 1857 which marked the beginning of contemporary colloidal science [16,17], AuNPs have been produced in different shapes and sizes and have served as adjuvant agents in numerous diagnostic techniques and medical imaging modalities. Computed tomography (CT) is amongst the most prevalent modalities of medical imaging where the use of a contrast agent is fairly common [18]. This exact necessity of a contrast agent use raises the question of whether AuNPs could be of any supplementary use. The answer may occur by observing the current gold standard. The clinical practice often pertains to the use of barium sulfate suspensions or water-soluble aromatic iodinated compounds, with the latter being more prevalent for X-ray applications [19]. These drugs often come with a number of adverse effects, such as kidney dysfunction and allergic reactions [20,21]. Furthermore, they lack any targeting capacity and are rapidly swept away by human clearance mechanisms [22].

As an alternative, innovative contrast agents that enhance clarity, AuNPs, have been created thanks to recent breakthroughs in nanotechnology. Since gold has a larger Z number than iodine, it attenuates X-rays more efficiently and generates greater resolution. Interestingly, AuNPs have a prolonged biological half-life more so than iodine-based compounds because of their high molecular weight [23]. Research has shown that size has an impact on X-ray attenuation. Compared to either bigger AuNPs or Omnipaque, which is a commercially available iodinated contrast agent, the smaller AuNPs (4 and 20 nm) exhibit greater X-ray attenuation. This feature can be attributed to the fact that smaller nanoparticles present a larger targeted surface area for X-rays [24]. Similar results were obtained by Dong et al., who proved that larger gold nanoparticles, ranging in size from 50 to 152 nm, exhibited better liver and spleen contrast [25].

Furthermore, AuNPs' ability to be coupled with various ligands can be utilized for active targeting. According to the experimental study of Popovtzer et al., gold nanorods were conjugated with UM-A9 antibodies to target squamous cell carcinoma in head and neck cancer. Thus, the images managed to offer adequate discrimination among healthy and cancerous cells, as depicted in Figure 1 [26].

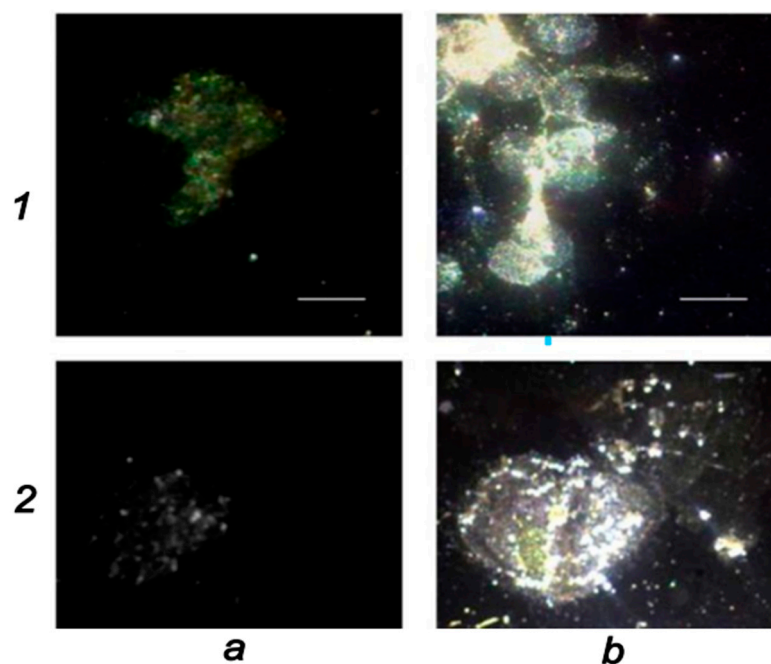


**Figure 1.** Dark field microscopy depiction of (1) oral SCC head and neck cancer cells, (2) larynx SCC head and neck cancer cells after incubation with (a) non-matching antibody-coated gold nanorods and (b) matching UM-A9 antibody-coated gold nanorods at a scale bar of 10  $\mu\text{m}$ . Reprinted with permission from reference [26]. Copyright © 2008, ACS Publishing.

Similarly, to overcome limitations in detecting liver tumors, heparin-coated AuNPs were employed, and images were developed successfully. The size of the newly formed heparin-coated AuNPs in an aqueous environment was  $54.6 \pm 19.6$  nm. It was discovered that HEPA-AuNPs presented high liver selectivity in lab animals due to the contrast acquired from the nanoparticle's use, with a duration up to 24 h. Nevertheless, it is worth mentioning that a large dosage of AuNPs was required for better X-ray uptake, which raises the concern of possible toxic effects [27]. Additionally, regarding AuNPs' stability, polymers could also be put to use. According to the research team of Sun et al., surface functionalization with biocompatible glycol chitosan may offer images presenting sharp contrast equivalent to that of a standard CT contrast medium. It is suspected that the incorporation of chitosan caused these hybrid NPs to be selectively absorbed by colon cancer cells. Interestingly, X-ray absorbance was not affected in the presence of these polymers [28]. When Ashton et al. compared the addition of full-sized antibodies (C225-AuNPs) with PEGylated AuNPs, they came to some interesting conclusions. Despite their shorter distribution period, tumor accumulation was substantially higher with antibody-conjugated AuNPs. This is an interesting example of strong binding affinity, which was more than sufficient to offset the negative consequences of larger nanoparticles (68 nm) on overall tumor accumulation [29].

Photoacoustic imaging (PA) is an innovative form of medical imaging that integrates the great spatial resolution of ultrasound imaging with the spectroscopic-based sensitivity of optical imaging [30]. AuNPs are capable of being used in dual imaging, combining PA and CT. Prussian blue (PB) was used to encapsulate AuNPs. In terms of improving X-ray CT imaging, the gold core works as a contrast agent. In PA imaging, the external PB shell acts as a potent NIR light absorber. The Au-PB NPs' size in an aqueous environment was determined to be  $17.8 \pm 2.3$  nm. The increase in Au-PB NP concentration resulted in an increase in the PA signal, suggesting significant PA contrast capability to identify the precise structure of the tumor sites paired with the optimal capabilities of Au, meaning that this probe could be ideal for cancer imaging [31]. In a similar manner, Cheheltani et al. produced biodegradable poly-di(carboxylatophenoxy)phosphazene (PCPP) gold nanospheres in an effort to obtain biocompatible contrast agents that could be applied in dual imaging. Figure 2 illustrates how the polymeric coating safeguards against rapid elimination and can gradually break down into biocompatible components and AuNPs after use, reducing the strain on the kidneys [18].

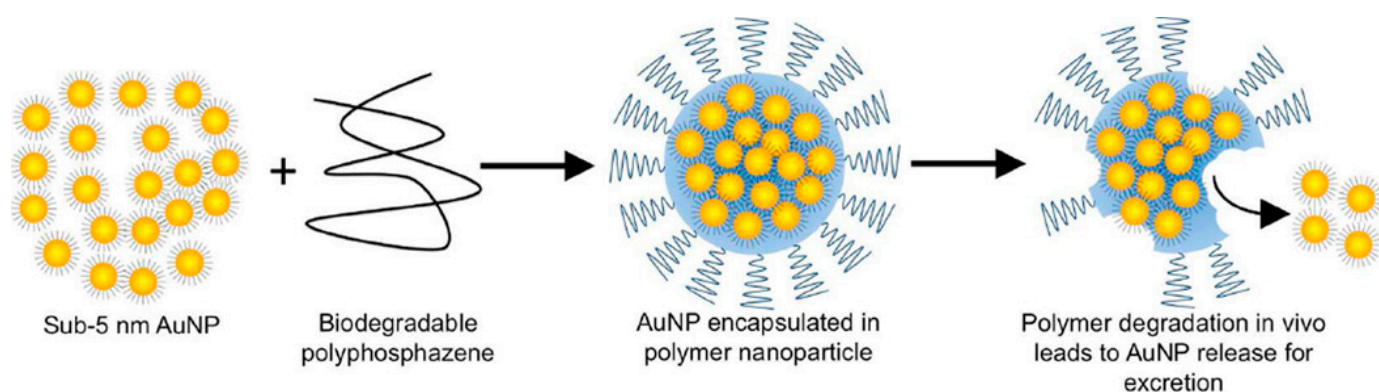


**Figure 2.** Illustration of biodegradable gold nanoparticles where 5 nm AuNPs can be incorporated into a biodegradable polyphosphazene (PCPP) and, thus, lead into the creation of larger NPs with a potentially increased imaging contrast agent which can degrade in vivo and excrete the 5 nm AuNPs. Reprinted with permission from reference [18]. Copyright © 2016, Elsevier.

The significance of size is demonstrated in Chen et al. Due to improved distribution, selectivity, thermal stability, and surface-to-volume ratio, targeted gold nanorods (W:  $8 \pm 2$  nm and L:  $49 \pm 8$  nm) exhibit an  $\times 4.5$  increase in tumor photoacoustic signal in animal experiments as opposed to their larger equivalents [32].

## 2.2. Gold Nanoparticles in Therapy

Various scientific groups have observed that due to AuNPs' strong photoelectric photon absorption, their use can drastically increase local dose deposition after being irradiated with kilovoltage (kV) photon energies or even polyenergetic megavoltage (MV) photon energies. This process leads to the emission of secondary radiation and to a subsequent cascade of low energy photoelectrons and Auger electrons. The showers of those low-energy (<5 keV) and short ranged (within a few  $\mu\text{m}$ ) electrons can prove to be very effective in damaging the DNA directly and in ionizing the surrounding water molecules. Thus, the combination of ionizing radiation of precise energy, type, and dose in consolidation with high-Z NPs of certain size, shape, and concentration can lead to localized enhancement of tumor radiosensitization and targeted lethal cell damage. More precisely, multiple radiation factors, such as the radiation dose, dose rate, fractionation scheme, and radiation source, would constitute a crucial factor for defining the optimum tumor response after irradiation. To mention just a few, it has been observed that the biological processes known as the four R's of radiation biology (repopulation, reoxygenation, redistribution, and repair) are strongly dependent upon the fractionation and dose rate [33–35]. Furthermore, it is well analyzed how radiation dose affects the level of radiation-induced damage or immunization [33,35–37].

Furthermore, the radiosensitization mechanism is usually correlated with reactive oxygen species (ROS) overproduction in the presence of AuNPs [33,38,39]. Thus, it would be interesting to analyze the effect from the perspective of gold NPs' catalytic activity. Unfortunately, AuNPs' ability to catalyze reactions which pertain to free radicals is yet not fully investigated. In general, AuNPs' toxicity is highly correlated with higher ROS production in their presence with and without ionizing radiation [40–42]. The research work of Shcherbakov et al. attempted to study AuNPs' catalytic effect on 2-propanol oxidation and acetanilide hydroxylation in aqueous solutions under ionizing radiation at room temperature [42]. They observed that the use of AuNPs initiated the selective oxidation of organic radicals and, thus, reached conclusion that AuNPs' catalytic activity could indeed influence the concentration of ROS [42].

In general, AuNPs constitute an alluring and promising research option towards cancer therapeutic methodologies, such as photodynamic therapy (PDT) [43] or photothermal therapy (PTT) [43], or even clinically useful applications, such as biosensors, targeted drug delivery, and immunoassays. Part of AuNPs' potential is illustrated in Figure 3 [43]. The fact that several types of AuNPs, such as nanospheres, nanorods, nanocubes, nanocages, and nanostars, present high effectiveness in the fields of cancer and cellular biology constitutes an interesting and encouraging factor [43].

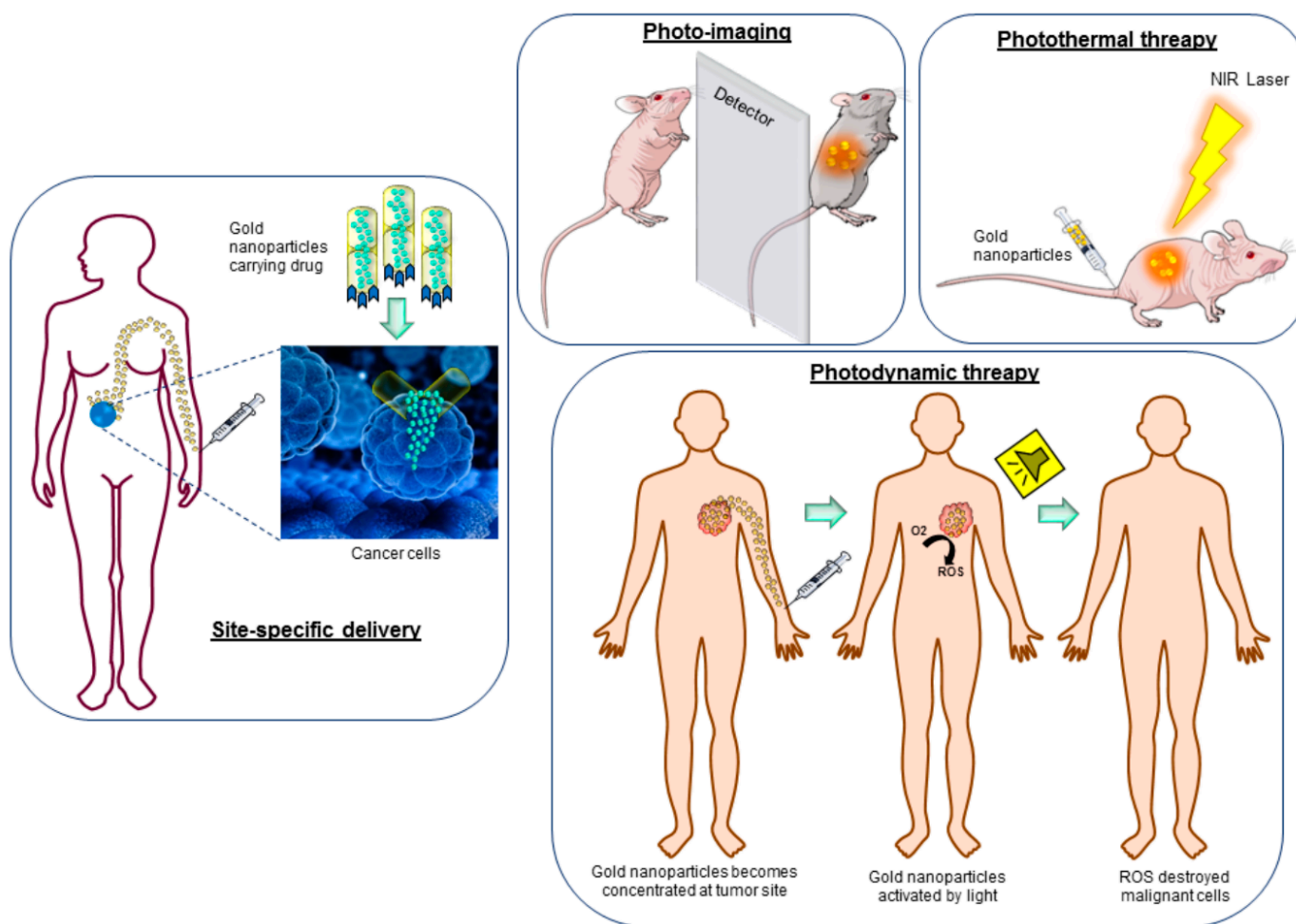


**Figure 3.** Possible applications of AuNPs in cancer therapy [43].

Consequently, the variety of physical, chemical, and biological mechanisms involved in the interactions of high-Z nanoparticles in cancer therapy leads to a variety of possible applications but, at the same time, to a significantly multifactorial experiment. Without a doubt, the optimal parameters for their function are still under investigation by the research community.

Regarding the nanoparticle size or the targeting ligand and their effects depending on the various cancer cell lines, the research of Luo et al. presents interesting results. The team simultaneously investigated the effect of AuNP size and surface ligands on cellular uptake, tumor targeting and radiotherapy efficiency for prostate cancer cell lines of PC3pip and PC3flu. AuNPs of different core sizes, namely 2 nm, 5 nm, and 19 nm, in addition to 7 nm of PEGylated NPs, were employed at a concentration of  $60 \text{ mg} \cdot \text{mL}^{-1}$ . The NPs were irradiated with X-rays at the doses of 0, 2, 4, and 6 Gy, followed by an incubation period before the final assessment of the tumor cell viability and the changes in tumor cell colony formation. Both bare and prostate-specific membrane antigen (PSMA)-conjugated AuNPs were used as radiosensitizers. The ligand conjugations were proven to increase the specific uptake of AuNPs of all sizes, rendering the conjugation significant for radiotherapy [44]. The experimental scheme is depicted in Figure 4.

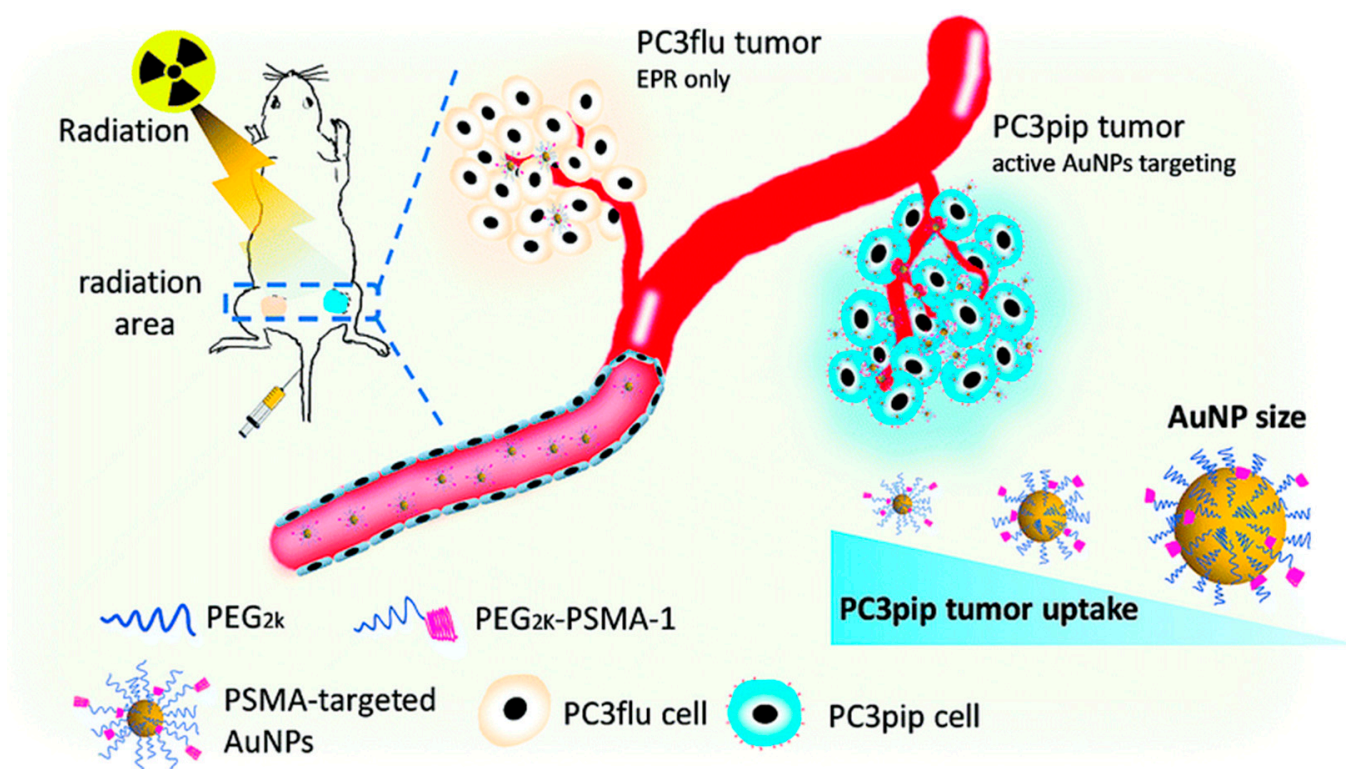


**Figure 4.** Depiction of targeted radiotherapy with the aid of PSMA-targeted AuNPs of different sizes for prostate cancer. Reprinted with permission from reference [44]. Copyright 2019, The Royal Society of Chemistry.

AuNP uptake was increased (a) in PC3pip cells after ligand conjugation, (b) in vivo when they were smaller, and (c) in vitro when they were larger [44]. In the absence of radiation (0 Gy) AuNPs had no toxic effect on the prostate cancer cells, but when the dose increased from 2 Gy to 6 Gy, PC3pip cell viability drastically deteriorated for all AuNP sizes [44]. Radiation enhancing factor (REF) was used to study the effect of AuNP size on radiation enhancement for all X-ray doses and despite smaller AuNPs obtaining inferior gold content per cell, they achieved superior radiation enhancement at 2, 4, and 6 Gy [44].

Farahani et al. compared the dose enhancement factor (DEF) of AuNPs of different radiation sources. More specifically, Co-60 was used at 1.25 MeV for external beam radiotherapy and Ir-192 for brachytherapy at 380 keV to irradiate MADAT polymer gel dosimeters doped with 0.2 mM AuNP [45]. During Ir-192 brachytherapy, gel tubes were irradiated at distances of 2.25, 3.75, and 5.25 cm with doses between 3.17–9 Gy, and external radiation therapy of the gel tubes was performed at 70 cm, with doses between 0–10 Gy [45]. Radiation-induced relaxation rate changes ( $R2 = 1/T2$ ) were detected by MR imaging and showed a significantly higher dose enhancement of  $15.31\% \pm 0.30$  for AuNP irradiated by Ir-192 versus a dose enhancement of  $5.85\% \pm 0.14$  for AuNPs irradiated by Co-60 [45].

Konefal et al. simulated (via the Monte Carlo method) three different AuNPs: a 50 nm nanorod (10 nm diameter), a 30 nm nanorod (5 nm diameter), and a two-dimensional nanostructure (30 nm × 30 nm × 0.1 nm). A LINAC was used to deliver 6 MV and 18 MV radiotherapeutic X-ray beams, at distances of 1.5 cm and 3.5 cm, respectively, to the target volume (with and without AuNPs) in a water phantom [46]. A dose increase was observed with the increase in mass concentration of gold in the nanoparticles for all shapes and both nanorod sizes; however, two-dimensional AuNPs provided superior in terms of radio-enhancement with external radiation therapy compared to the nanorods for both 6 MV and 18 MV X-ray irradiation [46].

Tudda et al. achieved a significant dose enhancement via AuNPs during rotational radiotherapy of MDA-MB-231 breast cancer cells using X-ray beam kV photons [47]. A total of 15 nm AuNPs of 100  $\mu\text{g}/\text{mL}$  (4.87 nM) and 200  $\mu\text{g}/\text{mL}$  (9.74 nM) were prepared for radiosensitization of the cancer cells, which were subjected to 100 kV, 190 kV, and 6 MV X-rays [47]. Following irradiation up until 2 Gy, cells incubated with AuNPs showed a decrease in viability compared to the cells without AuNPs, while the most significant radiosensitization effect was observed at the concentration of 9.74 nM, with the 190 kV beam obtaining a DEF of  $1.33 \pm 0.06$  [47].

Yogo et al. points out the necessity for decreased AuNP concentrations during radio-enhancement for clinical implementation to be feasible; thus, they investigated the effect of positively charged 1.4 nm AuNPs with MV X-rays on DNA damage and found a DEF of  $1.4 \pm 0.2$  and  $1.2 \pm 0.1$  for ssDNA- and dsDNA-breaks, respectively [48]. Positively charged AuNPs was proven to be more effective radiosensitizers than negatively charged AuNPs in the presence of MV X-ray beams and could potentially improve radiotherapy outcomes [48].

As has been already presented, the role of AuNPs as radiosensitizers in radiation therapy is significantly influenced by their size, shape, concentration, and surface coating. The literature review indicated that the effect of various AuNP concentrations regarding dose enhancement is significantly greater than the effect of their size [49]. The effect of AuNP size on radiation enhancement is due to smaller AuNP sizes having a greater surface area to volume ratio, allowing for more nanoparticle to cell atom interactions; however, small AuNPs are eliminated faster than larger ones by the kidneys, thus, limiting the duration of their radiosensitizing effect. On the other hand, increased AuNP concentrations mean a greater number of nanoparticle atoms are available and, therefore, more radiosensitizing interactions occur between target cells and AuNPs, thus, limiting cell growth rates [49]. The research team of McMahon et al. focused on the localized dosage enhancement due to the concentration or the AuNP size, and their results, among others, indicated that AuNPs in the shape of solid spheres present sufficient results [50]. Of course, the inhomogeneous distribution of AuNPs' concentration inside the tumor was taken into consideration, and it was proven that the density and material composition change according to the concentration of AuNPs inside the tumor region. Finally, the team concluded that the dose enhancement factor (DEF) increases approximately linearly with the concentration of gold nanoparticles. The limitations account for the toxicity. Hainfeld et al. examined different NP concentrations and observed that the concentration of 10 mg Au/g caused no detectable harm [51]. The team examined a 70 mg Au/g concentration of AuNPs to better illustrate the impact of concentration in comparison with DEF values [51]. However, in clinical radiotherapy, the use of such concentrations would be prohibited due to the increased toxicity. Indeed, more recent studies have shown that lower NP concentrations are much more effective. Rahman et al. studied the effect of different concentrations of AuNPs on enhancing radiosensitivity. This resulted in DEFs of 2.4 and 2.0 for 1 mM and 0.5 mM at 80 kVp, respectively. Furthermore, DEFs of 2.2 and 1.4 were collected for 1 mM and 0.5 mM at 150 kVp [52]. In specific types of malignancies, such as glioblastomas, research teams have yielded favorable results while utilizing lower concentrations of NPs. Guerra et al. experimented with concentrations of 20–500  $\mu\text{g}/\text{mL}$  on U87 glioblastoma cell lines [53].

### 3. Gadolinium Nanoparticles

Gadolinium is a rare-earth metal and a member of the lanthanide series. In terms of its physical characteristics, it is a moderately ductile, moderately hard, silvery-white metal that is quite stable in the air. With time, it degrades, forming a thin film of  $\text{Gd}_2\text{O}_3$  on the surface due to its oxidation [54].

Gadolinium NPs are black and spherical, and are commonly constructed in two average sizes, that of 10–45 nanometers with specific surface area in the 30–50  $\text{m}^2/\text{g}$  range, and that of the 75–90 nm range, with a specific surface area of approximately 5–10  $\text{m}^2/\text{g}$  [55]. Regarding their shape, GdNPs are available as nanorods, nanowhiskers, nanohorns, nanopy-

ramids, and other nanocomposites [55]. It is important to mention that Gd toxicity may limit its application in biomedical fields. Consequently, Gd is stabilized with diethylenetriaminepentaacetic acid (DTPA), forming a relatively inert and biocompatible clinical contrast agent, Gd-DTPA [56].

### 3.1. Gadolinium Nanoparticles in Medical Imaging

GdNPs seem to have the potential of becoming the next generation of contrast agents. In general, the ions of Gd show great water stability and excellent biocompatibility, while their longitudinal water proton spin relativity is significantly high [57]. Due to their tiny size and large specific surface area, GdNPs constitute excellent candidates for targeted cancer imaging with immense and selective levels of accumulation [58]. Numerous studies involving GdNPs have found that these NPs are typically conjugated with other chemical compounds or elements.

What makes gadolinium complexes interesting in imaging is their ability to shorten the longitudinal relaxation time (T1) of water protons because of the metal ion's high magnetic moment and symmetric electronic ground state with the presence of seven unpaired electrons. The most representative class of contrast agents consists of polyaminocarboxylate complexes of Gd<sup>3+</sup> ions [59]. The ligands are multidentate, comprised of seven or eight donor atoms [59]. Due to this, they manage to restrain the release of free metal ions which present high toxicity and, thus, interfere with Ca<sup>2+</sup> pathways [59]. The coordination cage of the Gd<sup>3+</sup> ion is completed with 1–2 water molecules. Eventually, these water molecules are engaged with transferring the paramagnetic properties to the overall bulk water molecules through a chemical exchange [59]. Thereafter, the capability of a Gd chelate to affect the water proton relaxation rates is defined by the relaxivity value [59]. The concentration of the paramagnetic MRI reporter is directly proportional to the relaxation enhancement in a proton MR image. Finally, these agents can be utilized to carry out Gd quantification at the pathological tissue [59].

Thus, the widest application of GdNPs so far can be found in MRI imaging. This selection relies on the fact that GdNPs present R1 relaxation rates higher than commercial contrast agents while, simultaneously, the R2/R1 ratio is close to 1. Therefore, they offer high image quality and vast soft tissue contrast [60,61]. It is worth mentioning that, with the insufficient longitudinal relaxivity (R1) which often describes commercial contrast agents, in MRI imaging it is often required during clinical praxis to inject higher contrast agent doses to achieve adequate contrast enhancement [62]. Given this potential, the team of Cho et al. developed water-soluble Gd<sub>2</sub>O<sub>3</sub> nanoparticles in the form of nanoplates (2 to 22 nm in size and 1 to 2 nm in thickness). They observed that the longitudinal relaxivity (R1) of the 2 nm Gd<sub>2</sub>O<sub>3</sub> nanoplates ended up being 10 times higher than that of the commercially available Gd-DTPA (~50 mM·s<sup>-1</sup> vs. ~4 mM·s<sup>-1</sup>) [62]. Furthermore, the same research indicated that, due to the PAA–OA coating of the GdNPs, the toxicity levels remain low and, thus, offer an excellent candidate in T1 MR contrast agents [62].

Moreover, GdNPs possess an advantage for *in vitro* and *in vivo* imaging due to the effective contrast effect produced by Gd<sup>3+</sup> 7 unpaired electrons [63]. In the study of Catanzaro et al., GdNPs as a contrast agent in MRI were incorporated into polylactide-co-glycolide chitosan scaffolds with a 200–600 nm diameter and 50–80 μm thickness. These microparticles that the regulated GdNPs release enable the integration of cell scaffolding and imaging functions [64]. Similarly, in the study of Lu et al., hyaluronic acid was integrated with GdNPs to create a Gd/Ha composite using the facile method, which was then injected into a cartilage injury model (rabbits). The NPs are processed by the kidney and liver and eliminated from the body through urine, and they can serve as a potentially effective MRI contrast agent for enhanced identification of cartilage lesions, as can be seen in Figure 5 [65]. It was also shown that only 7% of the Gd leaked from the NPs, indicating that NPs are safe as contrast agents [65]. However, the research team still proposes that despite the safety of the intra-articular applications, further research into GdNPs is required [66].

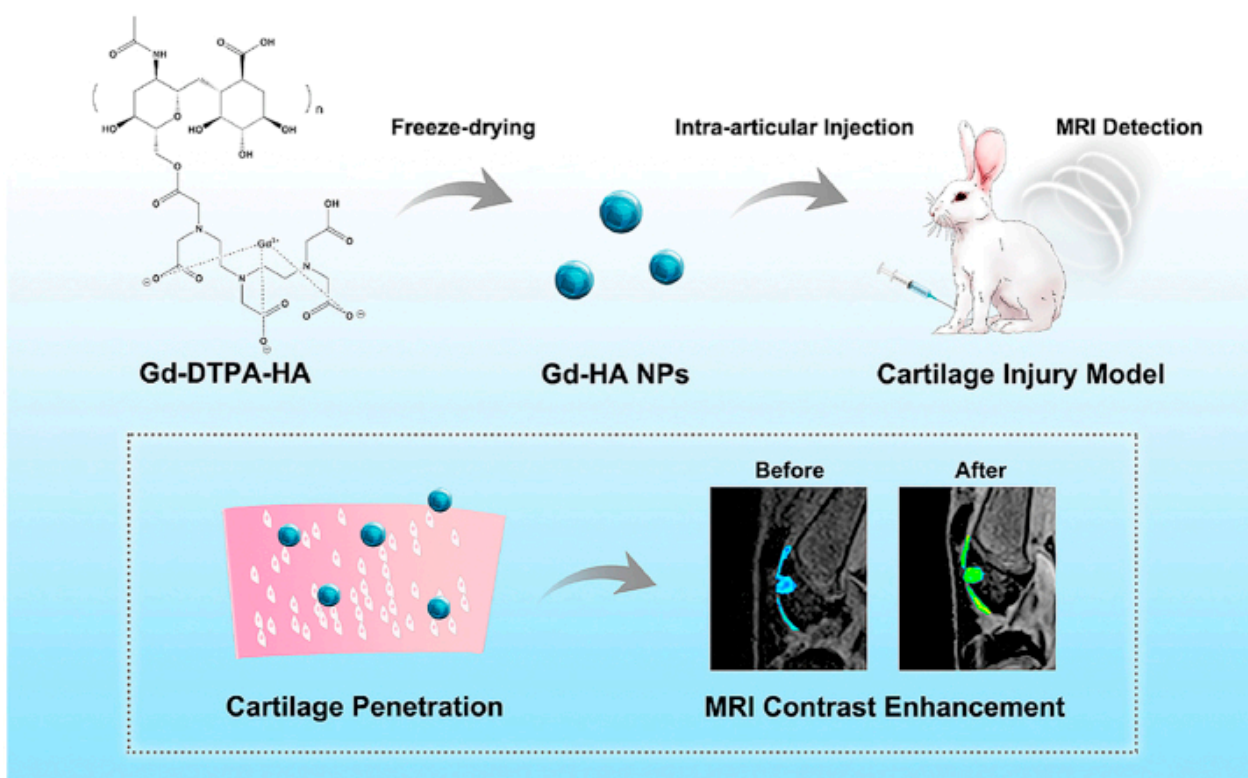


**Figure 5.** Schematic diagram of the application of Gd-HA NPs in the MRI detection of cartilage injuries [65]. Licensed under a Creative Commons Attribution-NonCommercial-NoDerivatives 4.0 International License.

Furthermore, in the study of Wu et al., when the GdNPs functionalized bismuth via a non-injection method, Gd-BiNPs appeared to have a round shape and a smooth surface. The hydrodynamic diameter was 45 nm and the polydispersity was 0.9. The results presented an MRI with a high X-ray attenuation coefficient and a short T1 relaxation time, but also a strong PAI signal [67]. Furthermore, the brightness and signal intensity of MR imaging increased as Gd concentrations increased [67]. Almost all studies have shown that Gd ions are toxic [57,60,61], so perhaps a conjugation of Au and Gd could reduce Gd ion leakage and improve system blood compatibility, resulting in extended circulation cycles and active targeting with minimal adverse effects. It is important to mention that all Gd-Cas can be administered intravenously. Due to this, it can be immediately equilibrate in the intravascular and interstitial compartments [68]. The excretion, based on different structures, is carried out by the liver or kidneys and depends upon passive diffusion or specific uptake processes [68]. The majority of Gd-Cas are granted at a dose of 0.1 mmol Gd/kg [68]. Finally, Gd contrast agents offered for clinical use are classified into (i) extracellular fluid agents, (ii) liver agents, and (iii) intravascular or blood pool agents [68].

### 3.2. Gadolinium Nanoparticles in Therapy

GdNPs, alone or conjugated with specific agents, have already shown promising results in different studies related to chemo-photodynamic, MRI-guided, photothermal, neutron-capture cancer therapy, and theranostic research.

A study showed a 96.6% tumor inhibition rate, and excellent MR imaging performance through a highly synergetic chemo-photodynamic antitumor effect in vitro and in vivo with the use of Gd/Pt bifunctionalized porphyrin derivative (Gd/Pt-P1) as a contrast agent. The platinum component served as a chemotherapeutic, and the Gd(III)-P1 complex played dual roles in both MR imaging and photodynamic therapy [69]. Porphyrin is a very effective chelate agent that has proven its functionality in chelating different metal ions [70–72]. Additionally, porphyrin has been studied in photodynamic therapy for its

attractive photo-physical properties [72–74]. More precisely, it has the ability to generate reactive oxygen species (ROS) by transferring photon energy to the molecular oxygen that is nearby and, subsequently, to destroy the cancer cells. Finally, porphyrin and its derivatives have been shown to selectively accumulate in tumor tissues. This serves to enable targeted cancer therapies [75–77]. Gd/Pt-P1 is localized in the nucleus, and this fact helps the agent to achieve its full potential in PDT. The study described previously showed minimal dark toxicity for C6 or COS-7 cells and, on the contrary, high photocytotoxicity. This ability is beneficial to tumor-specific PDT therapy with no side effects. Additionally, the study showed its efficacy compared to the commercial contrast agent “Magnevist” with high-quality MR imaging and effective PDT. These facts prove the Gd/Pt bifunctionalized porphyrin efficacy as a multifunctional theranostic agent with potential in MRI-guided cancer therapy [69].

Another study combined ultra-small GdNPs with trivalent gadolinium ions ( $Gd^{3+}$ ), functioning as absorptive agents, in order to enhance photothermal/photodynamic liver cancer therapy. Together they formed spherical self-assembled bodies of uniform size, were chemically coupled with matrix metalloproteinase-2, and were loaded with the photosensitive drug IR820.

Additionally, except for the successful enhancement of photodynamic/photothermal combination therapy, the potential for therapy guided by dual-mode real-time imaging of cancer has been proven due to the presence of MMP-2. The nanoparticles functioning as probes, T1 MRI, and in vivo fluorescence imaging modes showed excellent results. These nanoproboscopes can theoretically escape from the body due to their acid response degradation characteristics [78]. A study about gadolinium-conjugated gold nanoshells in multimodal diagnostic imaging showed their functionality as contrast agents in MRI, X-ray, and three optical imaging methods: OCT, RCM, and TPL. A significant improvement in MRI contrast was observed when gadolinium was conjugated to gold across a range of diagnostic modalities, with resolutions spanning anatomic to sub-cellular length scales. Furthermore, the particles were used for the enhancement of photothermal cancer therapy in a superficial melanoma tumor model, and it has been proven that they can efficiently ablate cancer cells in vitro when functioning as absorbers of NIR light. When this energy is converted to heat, it gains the ability to locally remove cancer tissue. More precisely, during the experiment, intratumoral injection of gadolinium-NS (50  $\mu$ L at  $6.3 \times 10^{12}$  NS/mL) in a subcutaneous B16-F10 melanoma tumor in a mouse was performed, and higher signal intensity was observed in tumor tissue under both T1-MRI and X-ray [79]. It is worth mentioning that the nanoparticles alone, without the radiation, did not harm the cells [79].

A gadolinium-based nanoparticle, AGuIX, 5 nm in size, which concentrates a high number of gadolinium atoms produced by NHT, has been proven effective as a theranostic and radiosensitizer agent in preclinical studies [80]. More precisely, the low toxicity was also presented in animal models, and its simple administration has initiated its first use in human study, the NANO-RAD study phase I [80]. The trial pertained to the first human injection, monocentric, open-label, dose-escalation study in order to access the side effects and safety for the use of AGuIX in combination with WBRT (30 Gy, 10 fractions of 3 Gy) for patients suffering from multiple brain metastases [80].

The research team of Verry et al. proceeded into the next step of the NANO-RAD study by delivering escalating doses of AGuIX NPs (of 15, 30, 50, 75, or 100 mg/kg intravenously) into patients with brain metastases combined with WBRT (30 Gy in 10 fractions) while simultaneously were assessing the toxicity levels [81]. They concluded that the combination of Gd-based AGuIX with radiotherapy constitute a safe option for patients, as the NP targets brain metastases and is retained within tumors for up to one week. In the meantime, phase II studies are ongoing [81].

#### Gadolinium Nanoparticles in Imaging-Guided Neutron Capture Therapy

GdNPs have been attracting scientific attention in the field of imaging-guided neutron capture therapy due to their high neutron cross-section (255,000 barns for the  $^{157}Gd$

isotope), which is approximately 65 times larger compared to the boron thermal neutron cross-section which also presents great interest (10 B) [82]. Despite this, unfortunately, the idea of GdNP use has been abandoned for years now due to the lack of appropriate tumor-selective gadolinium agents. Today, new gadolinium-containing compounds look very promising. Studies have been performed in many tumor animal models but, as of yet, none have been performed in human clinical trials. More specifically, the research group of Brugger [83] was one of the first to propose the application of gadolinium chelates as NCT agents for the treatment of brain tumors by intravenous injection of the agent. Kanda and colleagues reported the results of their application using a white rabbit with VX-2 tumors growing in their hind legs [84].

In general, the signal intensity enhancement of a T1-weighted MRI image is proportional to the Gd-based contrast agent concentration in the target tissue. Thus, by comparing images recorded before and after Gd contrast agent injection, it is possible to estimate Gd concentration at the pathological site and in other organs which could constitute the basis to set up NCT therapeutic protocols (with irradiation time and duration) as can be seen in Figure 6. This could lead to the facilitation of neutron irradiation optimization and, thus, to a reduction in damage to underlying healthy tissues. The lower thermal fluence in order to reduce the dose absorbed by normal tissues, as well as lower concentrations of the NCT agent, both compared to boron, with the latter reducing the tissue toxicity, make  $^{157}\text{Gd}$  a good potential theranostic agent. Nonetheless, limitations of the selectivity of the therapy using Gd-NCT, such as the emission of secondary  $\gamma$ -rays over a longer path length than boron, are to be considered. However, this limitation could transform into an advantage as the volume of the tumor increases by some  $\text{cm}^3$  [85].

It is worth mentioning that the intravenous administration of the agent has been proven to be the most efficient because it facilitates their accumulation in tumors, through active or passive targeting, leaving the surrounding tissues unharmed. With the aim of obtaining high intratumor concentrations of the agent, intratumor (500–1800 ppm) and peritumoral subdermal Gd injection (466 ppm) showed better outcomes [85].

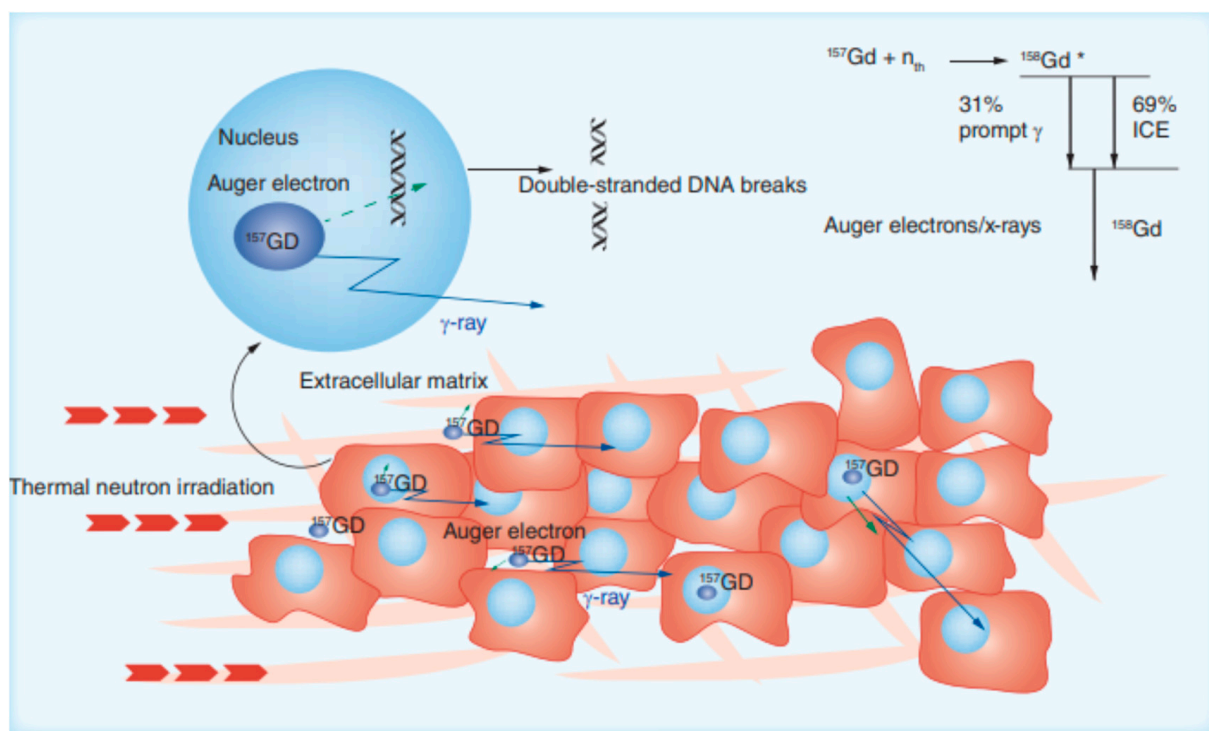


**Figure 6.** GdNP use in neutron capture reaction for therapeutic applications [85]. Copyright 2016, Future Medicine Ltd.

## 4. Consolidation of Gold and Gadolinium Nanoparticles

### 4.1. Applications in MRI

There are two ways to improve the resulting contrast of an MRI picture: (a) by enhancing the relaxivity of the contrast agent and (b) by increasing its concentration on-site [86]. The utilization of Gd chelates bound to gold nanoparticles is a promising alternative to existing agents in the MRI field as they cover both the aforementioned needs. The importance of chelating gadolinium to gold derives from the fact that Gd-based contrast agents have been associated with kidney malefaction, and free Gd cations stimulate an inflammatory response, resulting in scarring of the tissue [87].

The most commonly used method for binding Gd to a gold nanoparticle is the incorporation of a thiol moiety in the gadolinium chelate [86]. Cyclic disulfides, which form dithiolates on attachment to the surface [88], have also been applied as dithiocarbamates [89]. Dithiocarbamates have been shown to displace thiols on gold nanoparticle surfaces in a vigorous manner [90]. There are many chelators developed for connecting Gd to AuNPs, but the cyclic 10-tetraacetic acid (DOTA) is preferred due to its kinetic inertness [91]. An increase in the relaxation rate of water protons in their distribution area leads to an enhanced contrast between healthy and pathological tissues [92].

Meade et al. reported the strong connection of 2375 gadolinium chelates on the surface of 17 nm AuNPs by the formation of a dithiolate attachment at the gold surface. This connection was also responsible for restricting the motion of the chelates, resulting in increased relaxivity [93]. Fatehbasharзад et al. synthesized PEGylated (polyethylene glycol) gold nanospheres–gadolinium NPs (PEG-Gd@SPhGNPs) and PEGylated gold nanoconcave cubes–gadolinium NPs (PEG-Gd@CCNPs). Their study concluded that irregularly shaped NPs affect the second of the three spheres' contributions that, in paramagnetic systems, consist of the overall relaxivity of the system, according to the surface curvature. Additionally, they elongated the rotational correlation time of gadolinium. As a result, 13 times higher relaxivity than that of the currently used clinical contrast agents was observed. Of the two NPs, PEG-Gd@CCNPs had the highest relaxivity, making them a promising candidate for MRI contrast agent [94]. PEG is a widely used polymer that offers stability and biocompatibility to gold nanoparticles. In general, polymers added to the surface of nanoparticles prevent them from aggregating and camouflage them from the immune system, increasing their circulation time [86].

Chablotz et al. described the synthesis of an octadentate gadolinium unit based on DO3A with a dithiocarbamate tether, attached to the surface of AuNPs. The restricted rotation of the immobilized areas on the surface of the Gd complex led to a significant increase in relaxivity. This NP is an example of NPs created to deliver targeting imaging agents. The additional incorporation of surface units for biocompatibility (PEG and thioglucose units) and targeting units (folic acid) leads to little detrimental effect on the high relaxivity observed for these biocompatible materials [95]. Most importantly they appear to be capable of targeting the folate receptors overexpressed by cancer cells, such as HeLa cells, making them of increased significance and leading to an increased concentration of the contrast agent [95]. Aouidat et al. described a novel Gd–biopolymer–gold bimetallic NP system by complexing gadolinium to gold ions and infusing them in a biopolymer matrix. These Gd–gold NPs displayed hepatocytes in the liver as a result of their good cellular uptake. They also preserved T1 contrast inside the cells, providing a solid in vivo detection with T1 MRI [96].

Another simple tactic to enhance Gd concentration in a malignancy under examination is by exploiting the enhanced permeability and retention (EPR) effect that allows the Gd-functionalized nanoparticles to be accumulated in the tumor as a result of the leaky vasculature of the site. Therefore, a better definition is achieved, without harming the surrounding healthy tissues [97].

#### 4.2. Applications in Multimodal Imaging

Multimodal imaging agents have been developed to facilitate enhancement contrast in multiple modalities. The most important aspect of administering one multipurpose contrast agent is the avoidance of different biodistribution concerns [98]. Gadolinium–gold NP multimodal contrast agents have been applied for use in both MRI and CT, offering contrast enhancement [86].

For MRI/photoacoustic imaging, Xing et al. have synthesized a gold nanorod with surface-bound gadolinium chelated with an aspect ratio of 3:1. This NP was found to absorb light at 710 nm and a high relaxivity. An interesting fact was that the addition of a layer of 20 nm thick gadolinium oxysulfide (GOS) to gold nanorods with an aspect ratio of 2:2 improved the absorption wavelength of the nanorods to 818 nm [99]. Combining gadolinium ions to AuNPs coupled the fluorescent properties of the latter, generating multimodal contrast agents capable for use in MRI/fluorescence imaging [100]. For the case of MRI/single-photon emission computed tomography (SPECT), DOTA-based chelators were designed to encapsulate gadolinium ions on a gold nanoparticle platform. This technique can be expanded to include therapeutic radionuclides, offering a potential use in the field of theranostics [101].

Wenxiou Hou et al. established a method for synthesizing gold nanocluster GdNPs. In an aqueous solution, the gold nanoclusters were assembled into monodispersed spherical particles, and then electrostatic interactions between trivalent cations of gadolinium and negatively charged carboxyl groups on the GNCs were selectively induced, leading to the formation of NPs for use in tumor multimodal imaging. It is a simple and time-saving assembly procedure that allows the gadolinium ions to be chelated into the gold nanoparticles without using molecular Gd chelates. The GNC-GdNPs were studied for NIR/CT/MR imaging of A549 human non-small cell lung cancer cells *in vitro*, and showed great promise for future use in cancer diagnosis [102].

In the Benqing Zhou et al. study, polyethylene glycol (PEG) monomethyl ether-modified PEI was sequentially modified with Gd chelator and folic acid (FA)-linked PEG (FA-PEG) and was used as a template to synthesize AuNPs followed by Gd chelation and acetylation of the remaining PEI surface amines (FA-Gd-Au PENPs) for use as a nanoprobe for targeted dual mode tumor CT/MR imaging *in vivo*. They were found to be colloidal stable and cytocompatible in a given concentration range with targeting specificity, as well as the enhanced X-ray attenuation property and reasonable R1 relaxivity making them an excellent candidate for targeted tumor CT/MR imaging *in vivo* [103].

To evaluate the outcome of DC-based immunotherapies, the *in vivo* tracking of dendritic cell (DC) migration to the lymphatic system is essential. Cai Zang et al. designed a bimodal imaging agent, namely Au@Prussian blue-Gd@ovalbumin nanoparticles (APG@OVA NPs), for real-time tracking of the DC migration process by MRI. Moreover, surface-enhanced Raman scattering (SERS) pointed to the distribution of the colonized DCs in the lymphatic system at the single-cell level. DC activation was achieved by the exposed ovalbumin molecules on the NP before subcutaneous injection, while the Gb doped PB shells provided a background-free SERS signal and MRI signal simultaneously, resulting in APG@OVA NPs which were suitable for real-time tracking of the DC migration by MRI and reliable distribution information about the DCs colonizing the lymph nodes with SERS [104].

#### 4.3. Theranostic Agents

A theranostic agent provides the clinician with real-time information on the biodistribution of the drug within the body while delivering a treatment itself [86]. In photothermal therapy (PTT) gold nanostructures can be used as photothermal agents, as they are able to convert near-infrared radiation into heat energy due to their localized surface plasmon effect. Functionalizing the gold nanostructure with gadolinium chelates allows the formation of a theranostic agent for combined PTT and MRI [105]. Furthermore, silica-gold core-shell NPs have been synthesized with an orthopyridil disulfide linker to allow the attachment of

gadolinium chelates to the gold surface. The GdNPs are able to absorb NIR at 800 nm and, because of the gadolinium, they can achieve a relaxivity of  $37 \text{ mM}\cdot\text{s}^{-1}$  per Gd unit at 1.41 T for combined PTT and MRI [79]. In addition to this, gold nanostars have been used in vitro and preclinically as PTT agents [106]. The relaxivities of gadolinium chelates attached to nanostars are often far greater than those in equivalent nanosphere syntheses [86]. In the case of photodynamic therapy (PDT), photosensitizers have been attached to AuNPs to generate singlet oxygen, delivering cancer treatment [107]. In a notable study, a photosensitizer was attached to a gadolinium-functionalized gold nanoshell for combined MRI, CT, PTT, and PDT [108]. Referring to radiotherapy, use of gold nanomaterials has been made, since their electron-dense nature makes them strong absorbers of high-frequency electromagnetic radiation. Gold nanomaterials with gadolinium chelates allow scientists to assess the nanoparticle accumulation level by MRI prior to treatment, ensuring the maximum impact of the nanoparticles during radiotherapy [109].

Memona Khan et al. designed and formulated doxorubicin (DOX) gadolinium–gold complexes. Doxorubicin (DOX), an anticancer therapeutic agent, was loaded on bimetallic gold nanorods in which gold salt ( $\text{HAuCl}_4$ ) was chelated with anthracycline (DOX), diacid polyethylene glycol (PEG-COOH) and gadolinium salt ( $\text{GdCl}_3 \cdot 6 \text{H}_2\text{O}$ ). Two NPs were formed depending on the placement of DOX: DOX ON-Gd-AuNRs, with DOX conjugated onto the Gd-AuNRs, and DOX IN-Gd-AuNRs, with DOX placed inside the Gd-AuNRs. The results showed that PTT was achieved at 808 nm in the NIR transparency window, cytotoxicity was observed toward tumoral MIAPaCa-2 cells, and MRI T1 features at 7T enabled interesting positive contrast for bioimaging [110].

Muhammad Sani Usman et al. developed gadolinium-based theranostic nanoparticles as contrast agents for MRI and for the co-delivery of drugs. They used Zn/Al-layered double hydroxide as the nanocarrier platform, gallic acid (GA) as the therapeutic agent, and  $\text{Gd}(\text{NO}_3)_3$  as the diagnostic agent, while AuNPs were grown on the system to form the Gd-based nanocomposite (GAGZAu). The in vitro drug release study presented higher drug release in pH 4.8 (the pH of cancer cells), indicating the capability of the platform to deliver the GA into cancer cells and prevent a bloodstream premature release. Reasonable cytotoxicity to HepG2 cancer cell lines and negligible toxicity to 3T3 normal cell lines was achieved. The NP also developed an improved MRI contrast in the T1-weighted image obtained as compared to pure  $\text{Gd}(\text{NO}_3)_3$  and water [111].

The same team a year later published a new study about the synthesis of a bimodal theranostic nanodelivery system (BIT) based on graphene oxide, chlorogenic acid as the anticancer agent, and gadolinium–gold nanoparticles (GOGCA) as contrast agents for MRI. About 90% of the chlorogenic acid was released from GOGCA under acidic cancer pH, which suggests high delivery in the cancer location. The nanoparticle was observed to have increased the contrast of the T1-weighted image tested by MRI and, interestingly, showed a higher signal than the conventional MRI contrast agent ( $\text{Gd}(\text{NO}_3)_3$ ), giving promising results for a holistic cancer medication in the future [112].

Lu Han et al. produced a protein-stabilized multifunctional theranostic nanoplatfrom, a gadolinium oxide–gold nanoclusters hybrid ( $\text{Gd}_2\text{O}_3$ -AuNCs), for multimodal imaging and drug delivery. The nanocomposites were water-dispersible, biocompatible, and were able to generate singlet oxygen species under NIR laser irradiation for photodynamic therapy. They were also able to present high loading capacity for the therapeutic agent indocyanine green (ICG). The NP demonstrated excellent triple-modal near-infrared fluorescence/magnetic resonance/computed topography (NIRF/MR/CT) imaging capability, as well a combined photodynamic and photothermal effectiveness [113].

#### 4.4. Applications in Cancer Treatment

Roux et al. developed the Au@DTDTPA(Gd) nanoparticles, i.e., original ultra-small nanoparticles comprised of a gold core and dithiolated polyaminocarboxylate shell doped with gadolinium ions, and then demonstrated their relevance and their potential for

MRI-guided radiation therapy. In particular, preclinical experiments demonstrated that Au@DTDTPA(Gd) could be of interest for the management of brain tumors [114].

Durand et al. study pointed out a noticeable decrease in glioma cell invasiveness when tumor cells were exposed to Au@DTDTPA(Gd) nanoparticles. Au@DTDTPA(Gd) nanoparticles affected the intrinsic biomechanical properties of U251 glioma cells, such as cell stiffness, adhesion, and generated traction forces, and significantly reduced the formation of protrusions, thus, exerting an inhibitory effect on their migration capacities. The results showed that the Au@DTDTPA(Gd) nanoparticles could have great interest for the therapeutic management of astrocytic tumors, not only as a radio-enhancing agent but also by reducing the invasive potential of glioma cells [115].

Bei Li et al. synthesized ultra-small gold nanoparticles induced with gadolinium ions forming a spherical self-assembly and coupled them with matrix metalloproteinase-2 (MMP-2); they were then loaded with the photosensitive drug IR820 (Gd–AuNPS@IR820) for photothermal/photodynamic combination therapy for liver cancer. Due to the presence of MMP-2, the nanoprobe showed excellent tumor-targeting properties in both T1 MRI and in vivo fluorescence imaging modes. In vivo treatment results fully prove that the nanoprobe has achieved satisfactory therapeutic effects after laser irradiation mediated photothermal/photodynamic combination treatment. The main organs of each treatment group did not show obvious pathological damage, proving that this nanoprobe has excellent in vivo biocompatibility [78].

The overview of the most recent applications in medical imaging and therapy of functionalized gold and gadolinium nanoparticles are depicted in Table 1.

**Table 1.** Consolidation of gold and gadolinium nanoparticles for medical applications in imaging and therapeutics.

Nanoparticle	Medical Application	Research Team
PEGylated gold nanospheres–gadolinium NPs (PEG-Gd@SPhGNPs)	MRI contrast agent	Fatehbasharзад et al. [94]
PEGylated gold nano concave cubes–gadolinium NPs (PEG-Gd@CCNPs)	MRI contrast agent	Fatehbasharзад et al. [94]
Gadolinium–biopolymer–gold bimetallic NP system	MRI contrast agent	Aouidat et al. [96]
Octadentate gadolinium unit based on DO3A with a dithiocarbamate tether, attached to the surface of gold NPs	MRI contrast agent	Chabloz et al. [95]
Gold nanorod with surface-bound gadolinium chelates	MRI/photoacoustic imaging agent	Qin et al. [99]
Gadolinium–gold nanocluster NPs	NIR/CT/MR imaging agent for A549 human non-small cell lung cancer cell imaging in vitro	Hou et al. [102]
Gadolinium chelated gold NPs–acetylated PEI surface amines (FA-Gd–Au PENPs)	CT/MR imaging agent in vivo	Zhou et al. [103]
Gold–Prussian blue–gadolinium ovalbumin nanoparticles (APG@OVA NPs)	MRI/surface-enhanced Raman scattering agent	Zhang et al. [104]
Doxorubicin (DOX) gadolinium–gold complexes (DOX ON-Gd–AuNRs) (DOX IN-Gd–AuNRs)	Photothermal therapy application/MRI agent	Khan et al. [110]

Table 1. Cont.

Nanoparticle	Medical Application	Research Team
Double-layered Zn/Al-gallic acid (GA)-gadolinium (NO <sub>3</sub> ) <sub>3</sub> -gold nanoparticles (GAGZAu)	Theranostic nanodelivery system (drug delivery system/MRI agent)	Sani Usman et al. [111,112]
Graphene oxide-chlorogenic acid-gadolinium-gold nanoparticles (GOGCA)	Theranostic nanodelivery system (drug delivery system/MRI agent)	Usman et al. [112]
Gadolinium oxide-gold nanoclusters hybrid (Gd <sub>2</sub> O <sub>3</sub> -AuNCs)	Theranostic nanoplatform (PDT application/drug delivery system/NIRF/MR/CT imaging agent)	Han et al. [113]
Gold core dithiolated polyaminocarboxylate shell doped with gadolinium ions (Au@DTDTPA(Gd))	MRI agent for guided radiation therapy of brain tumors	Debouttière et al. [116]
Spherical self-assembly of gold NPs-gadolinium ions-metalloproteinase-2-IR820 (Gd-AuNPS@IR820)	PDT/PTT application on liver cancer	Li et al. [78]

## 5. Challenges and Future Perspectives

The rapid expansion of nanotechnology has led to various applications in major fields. In biomedical applications, AuNPs have constituted the “golden standard” in research for many years, but also raise considerable challenges. One of the main concerns in biological systems is that of bioaccumulation, meaning the process through which an organism acquires a deposited substance. Thus, despite the undoubted benefits of gold nanoparticles, their biocompatibility remains a crucial issue. Even though their inert nature offers a relatively adequate biocompatibility, their cytotoxicity levels need to be further evaluated [43]. After all, until now, very few clinical trials involving gold nanoparticles for cancer therapy and diagnosis have received approval [43,117,118]. More precisely, in the field of medicine, the FDA has only granted approval for nanoparticle-based technologies aimed towards cancer therapy and diagnosis [43,96,119,120]. At this point, it is important to mention that NPs’ cytotoxicity has been proven to be highly dependent upon their size and morphology, shape, surface properties, method of production, and their chemical composition [43,119,120]. This raises the question of whether the consolidation of AuNPs with different chemical compounds, such as gadolinium, may reduce the toxicity levels and enhance the NPs’ efficiency.

However, it is crucial to consider any unintended side effects which may occur to human health. The challenges apart from toxicity include NP retention time, their level of efficacy, and the physiological response, as well as their biodistribution. The greatest challenge yet is that research still indicates that all these parameters seem to contradict one another. To sum up, there are still a variety of critical issues to be addressed regarding nanoparticles’ stability, long-term health effects, reliable manufacturing methods, and, of course, their cellular and immune responses.

Research on gold and gadolinium NPs so far indicates promising results towards their future applications. Studies that have evaluated novel nanotheranostic methods and break-through modalities, such as MR-LINAC systems, have shown that the consolidation of gold and gadolinium has been proven to enhance radiotherapy treatment while simultaneously strengthening the MR contrast [96]. Certainly, the combined magnetic resonance imaging with the linear accelerator systems is now enabling MRI-guided radiotherapy, which leads to the future perspective of an advanced workflow where the NP uptake during treatment as well as their effects could be confirmed by the MR image.

Nanoparticles morphology and their chemical ability of functionalization promise to play a crucial role in the future applications of nanomedicine. For instance, AuNPs in the shape of nanorods demonstrate lower levels of toxicity, outstanding optical properties and convenient surface chemical functionalization compared to other AuNPs [110,121,122]. The

research team of Khan et al. developed a novel GdNP complexed to gold ions and a PEG biopolymer matrix conjugated with antitumoral doxorubicin which could significantly assist in the theranostic field [110]. Through the tailoring of the GdNPs' morphology, they managed to increase the cytotoxicity localized to the tumor cells and, due to the NPs' adaptive size, they observed enhanced passive targeting to cancerous cells by enhanced permeability retention [110]. Furthermore, the construction of this unique GdNP offered a positive contrast in MRI bioimaging [110]. Thus, it is encouraging to believe that NPs' morphology will constitute a key factor towards their imaging and antitumoral properties in the future studies of medical applications against cancer.

Furthermore, future improvements include designing new gadolinium carriers in order to fully exploit the toxic effect generated by Au electrons, as well as the use of targeting vectors that deliver gadolinium-NCT only to tumor cells. Additionally, personalization of neutron therapy by in vivo biodistribution in the tumor by MRI can be detected in real-time. Furthermore, the use of the  $^{157}\text{Gd}$  enriched isotope will reduce the gadolinium concentration necessary to obtain a significant therapeutic result. Additionally, combining boron and gadolinium to improve the therapeutic efficacy, and combining Gadolinium-NCT with synergic therapeutic strategies with the coadministration of other antitumor agents, such as doxorubicin or pemetrexed, will also be beneficial [95].

## 6. Conclusions

Gold nanomaterials have been in the spotlight of the research community for many decades now. Their use has presented valuable results and has classified them as a valuable weapon against cancer. However, the range of their proper clinical applications in medical imaging and therapy are only now being realized. The recent developments highlighted in this review suggest a bright future for gadolinium-functionalized gold nanomaterials in therapy, multimodal imaging, and theranostics. Their combination could decrease or even prevent unwanted clinical consequences for the patient such, as gold's increased toxicity, and eventually lead to a safer, more stabilized, and longer-circulating nanoparticle. Phenomena, such as aggregation and agglomeration, can be restrained, leaving the beneficial results of NPs as localized dose enhancers targeted in cancer cells. Furthermore, gadolinium functionalized AuNPs could finally generate a multimodal contrast agent capable of providing clinical real-time information on disease progression, which simultaneously acts as a therapeutic agent. That way, the consolidation of gold and gadolinium NPs could assist in the field of theranostics. Certainly, this rich field of research requires further investigation and thorough study before reaching the level of approved clinical use. Hopefully, the following years of research will reveal the yet unknown potential of gold and gadolinium NPs, and will successfully set them in the medical quiver.

**Author Contributions:** Conceptualization, E.P.E. and M.A.K.; writing—original draft preparation, K.P., G.L., A.M., I.-A.V., A.M.G. and M.A.K.; writing—review and editing, K.P., G.L., A.M., I.-A.V., A.M.G., M.A.K. and E.S. All authors have read and agreed to the published version of the manuscript.

**Funding:** This research received no external funding.

**Data Availability Statement:** Not applicable.

**Acknowledgments:** This review was conducted in the Frame of Master Program entitled "Nanomedicine" for the academic year 2021–2022.

**Conflicts of Interest:** The authors declare no conflict of interest.

## References

1. Martin, T.A.; Ye, L.; Sanders, A.J.; Lane, J.; Jiang, W.G. Cancer invasion and metastasis: Molecular and cellular perspective. In *Madame Curie Bioscience Database*; Landes Bioscience: Austin, TX, USA, 2013.
2. Siddique, S.; Chow, J.C.L. Recent Advances in Functionalized Nanoparticles in Cancer Theranostics. *Nanomaterials* **2022**, *12*, 2826. [[CrossRef](#)] [[PubMed](#)]

3. Ojha, A.; Jaiswal, S.; Bharti, P.; Mishra, S.K. Nanoparticles and Nanomaterials-Based Recent Approaches in Upgraded Targeting and Management of Cancer: A Review. *Cancers* **2023**, *15*, 162. [[CrossRef](#)] [[PubMed](#)]
4. Sharifi, S.; Behzadi, S.; Laurent, S.; Forrest, M.L.; Stroeve, P.; Mahmoudi, M. Toxicity of nanomaterials. *Chem. Soc. Rev.* **2012**, *41*, 2323–2343. [[CrossRef](#)] [[PubMed](#)]
5. Mueller, R.; Moreau, M.; Yasmin-Karim, S.; Protti, A.; Tillement, O.; Berbeco, R.; Hesser, J.; Ngwa, W. Imaging and Characterization of Sustained Gadolinium Nanoparticle Release from Next Generation Radiotherapy Biomaterial. *Nanomaterials* **2020**, *10*, 2249. [[CrossRef](#)] [[PubMed](#)]
6. Nosrati, H.; Salehiabar, M.; Charmi, J.; Yaray, K.; Ghaffarlou, M.; Balcioglu, E.; Ertas, Y.N. Enhanced In Vivo Radiotherapy of Breast Cancer Using Gadolinium Oxide and Gold Hybrid Nanoparticles. *ACS Appl. Bio Mater.* **2023**, *6*, 784–792. [[CrossRef](#)]
7. Wu, C.; Cai, R.; Zhao, T.; Wu, L.; Zhang, L.; Jin, J.; Xu, L.; Li, P.; Li, T.; Zhang, M.; et al. Hyaluronic Acid-Functionalized Gadolinium Oxide Nanoparticles for Magnetic Resonance Imaging-Guided Radiotherapy of Tumors. *Nanoscale Res. Lett.* **2020**, *15*, 94. [[CrossRef](#)]
8. Ertas, Y.N.; Jarenwattananon, N.N.; Bouchard, L.-S. Oxide-Free Gadolinium Nanocrystals with Large Magnetic Moments. *Chem. Mater.* **2015**, *27*, 5371–5376. [[CrossRef](#)]
9. Horiguchi, Y.; Kudo, S.; Nagasaki, Y. Gd@C82 metallofullerenes for neutron capture therapy—Fullerene solubilization by poly(ethylene glycol)-block-poly(2-(N, N-diethylamino) ethyl methacrylate) and resultant efficacy in vitro. *Sci. Technol. Adv. Mater.* **2011**, *12*, 44607. [[CrossRef](#)]
10. You, Q.; Sun, Q.; Yu, M.; Wang, J.; Wang, S.; Liu, L.; Cheng, Y.; Wang, Y.; Song, Y.; Tan, F.; et al. BSA–Bioinspired Gadolinium Hybrid-Functionalized Hollow Gold Nanoshells for NIRF/PA/CT/MR Quadmodal Diagnostic Imaging-Guided Photothermal/Photodynamic Cancer Therapy. *ACS Appl. Mater. Interfaces* **2017**, *9*, 40017–40030. [[CrossRef](#)]
11. Li, D.; Wen, S.; Sun, W.; Zhang, J.; Jin, D.; Peng, C.; Shen, M.; Shi, X. One-Step Loading of Gold and Gd<sub>2</sub>O<sub>3</sub> Nanoparticles within PEGylated Polyethylenimine for Dual Mode Computed Tomography/Magnetic Resonance Imaging of Tumors. *ACS Appl. Bio Mater.* **2018**, *1*, 221–225. [[CrossRef](#)]
12. Roy, A.; Pandit, C.; Gacem, A.; Alqahtani, M.S.; Bilal, M.; Islam, S.; Hossain, J.; Jameel, M. Biologically Derived Gold Nanoparticles and Their Applications. *Bioinorg. Chem. Appl.* **2022**, *2022*, 8184217. [[CrossRef](#)]
13. Gehan, H.; Fillaud, L.; Felidj, N.; Aubard, J.; Lang, P.; Chehimi, M.M.; Mangeney, C. A general approach combining diazonium salts and click chemistries for gold surface functionalization by nanoparticle assemblies. *Langmuir* **2010**, *26*, 3975–3980. [[CrossRef](#)]
14. Ackerson, C.J.; Jadzinsky, P.D.; Jensen, G.J.; Kornberg, R.D. Rigid, Specific, and Discrete Gold Nanoparticle/Antibody Conjugates. *J. Am. Chem. Soc.* **2006**, *128*, 2635–2640. [[CrossRef](#)]
15. Pinter, B.; Broeckart, L.; Turek, J.; Růžička, A.; De Proft, F. Dimers of N-Heterocyclic Carbene Copper, Silver, and Gold Halides: Probing Metallophilic Interactions through Electron Density Based Concepts. *Chem.—A Eur. J.* **2014**, *20*, 734–744. [[CrossRef](#)]
16. Faraday, M.X. The Bakerian Lecture.—Experimental relations of gold (and other metals) to light. *Philos. Trans. R. Soc. Lond.* **1857**, *147*, 145–181.
17. Edwards, P.P.; Thomas, J.M. Gold in a Metallic Divided State—From Faraday to Present-Day Nanoscience. *Angew. Chem. Int. Ed.* **2007**, *46*, 5480–5486. [[CrossRef](#)]
18. Cheheltani, R.; Ezzibdeh, R.M.; Chhour, P.; Pulaparthy, K.; Kim, J.; Jurcova, M.; Hsu, J.C.; Blundell, C.; Litt, H.I.; Ferrari, V.A.; et al. Tunable, biodegradable gold nanoparticles as contrast agents for computed tomography and photoacoustic imaging. *Biomaterials* **2016**, *102*, 87–97. [[CrossRef](#)]
19. Yu, S.-B.; Watson, A.D. Metal-Based X-ray Contrast Media. *Chem. Rev.* **1999**, *99*, 2353–2378. [[CrossRef](#)]
20. Bernstein, A.L.; Dhanantwari, A.; Jurcova, M.; Cheheltani, R.; Naha, P.C.; Ivanc, T.; Shefer, E.; Cormode, D.P. Improved sensitivity of computed tomography towards iodine and gold nanoparticle contrast agents via iterative reconstruction methods. *Sci. Rep.* **2016**, *6*, 26177. [[CrossRef](#)]
21. Nadolski, G.J.; Stavropoulos, S.W. Contrast alternatives for iodinated contrast allergy and renal dysfunction: Options and limitations. *J. Vasc. Surg.* **2013**, *57*, 593–598. [[CrossRef](#)]
22. Shilo, M.; Reuveni, T.; Motiei, M.; Popovtzer, R. Nanoparticles as computed tomography contrast agents: Current status and future perspectives. *Nanomedicine* **2012**, *7*, 257–269. [[CrossRef](#)] [[PubMed](#)]
23. Aydogan, B.; Li, J.; Rajh, T.; Chaudhary, A.; Chmura, S.J.; Pelizzari, C.; Wietholt, C.; Kurtoglu, M.; Redmond, P. AuNP-DG: Deoxyglucose-labeled gold nanoparticles as X-ray computed tomography contrast agents for cancer imaging. *Mol. Imaging Biol.* **2010**, *12*, 463–467. [[CrossRef](#)] [[PubMed](#)]
24. Xu, C.; Tung, G.A.; Sun, S. Size and Concentration Effect of Gold Nanoparticles on X-ray Attenuation As Measured on Computed Tomography. *Chem. Mater.* **2008**, *20*, 4167–4169. [[CrossRef](#)] [[PubMed](#)]
25. Dong, Y.C.; Hajfathalian, M.; Maidment, P.S.N.; Hsu, J.C.; Naha, P.C.; Si-Mohamed, S.; Breuilly, M.; Kim, J.; Chhour, P.; Douek, P.; et al. Effect of Gold Nanoparticle Size on Their Properties as Contrast Agents for Computed Tomography. *Sci. Rep.* **2019**, *9*, 14912. [[CrossRef](#)]
26. Popovtzer, R.; Agrawal, A.; Kotov, N.; Popovtzer, A.; Balter, J.; Carey, T.; Kopelman, R. Targeted Gold Nanoparticles Enable Molecular CT Imaging of Cancer. *Nano Lett.* **2008**, *8*, 4593–4596. [[CrossRef](#)]
27. Sun, I.-C.; Eun, D.-K.; Na, J.H.; Lee, S.; Kim, I.-J.; Youn, I.-C.; Ko, C.-Y.; Kim, H.-S.; Lim, D.; Choi, K.; et al. Heparin-Coated Gold Nanoparticles for Liver-Specific CT Imaging. *Chem.—A Eur. J.* **2009**, *15*, 13341–13347. [[CrossRef](#)]

28. Sun, I.-C.; Na, J.H.; Jeong, S.Y.; Kim, D.-E.; Kwon, I.C.; Choi, K.; Ahn, C.-H.; Kim, K. Biocompatible Glycol Chitosan-Coated Gold Nanoparticles for Tumor-Targeting CT Imaging. *Pharm. Res.* **2014**, *31*, 1418–1425. [[CrossRef](#)]
29. Ashton, J.R.; Gottlin, E.B.; Patz, E.F., Jr.; West, J.L.; Badea, C.T. A comparative analysis of EGFR-targeting antibodies for gold nanoparticle CT imaging of lung cancer. *PLoS ONE* **2018**, *13*, e0206950. [[CrossRef](#)]
30. Beard, P. Biomedical photoacoustic imaging. *Interface Focus* **2011**, *1*, 602–631. [[CrossRef](#)]
31. Jing, L.; Liang, X.; Deng, Z.; Feng, S.; Li, X.; Huang, M.; Li, C.; Dai, Z. Prussian blue coated gold nanoparticles for simultaneous photoacoustic/CT bimodal imaging and photothermal ablation of cancer. *Biomaterials* **2014**, *35*, 5814–5821. [[CrossRef](#)]
32. Chen, Y.-S.; Zhao, Y.; Yoon, S.J.; Gambhir, S.S.; Emelianov, S. Miniature gold nanorods for photoacoustic molecular imaging in the second near-infrared optical window. *Nat. Nanotechnol.* **2019**, *14*, 465–472. [[CrossRef](#)]
33. Her, S.; Jaffray, D.A.; Allen, C. Gold nanoparticles for applications in cancer radiotherapy: Mechanisms and recent advancements. *Adv. Drug Deliv. Rev.* **2017**, *109*, 84–101. [[CrossRef](#)]
34. Arnold, H. *Basic Clinical Radiobiology*, 4th ed.; CRC Press: London, UK, 2009.
35. Ahn, G.-O.; Brown, J.M. Matrix Metalloproteinase-9 Is Required for Tumor Vasculogenesis but Not for Angiogenesis: Role of Bone Marrow-Derived Myelomonocytic Cells. *Cancer Cell* **2008**, *13*, 193–205. [[CrossRef](#)]
36. Garcia-Barros, M.; Paris, F.; Cordon-Cardo, C.; Lyden, D.; Rafii, S.; Haimovitz-Friedman, A.; Fuks, Z.; Kolesnick, R. Tumor Response to Radiotherapy Regulated by Endothelial Cell Apoptosis. *Science* **2003**, *300*, 1155–1159. [[CrossRef](#)]
37. Dewan, M.Z.; Galloway, A.E.; Kawashima, N.; Dewyngaert, J.K.; Babb, J.S.; Formenti, S.C.; Demaria, S. Fractionated but not single-dose radiotherapy induces an immune-mediated abscopal effect when combined with Anti-CTLA-4 antibody fractionated radiation synergizes with immunotherapy. *Clin. Cancer Res.* **2009**, *15*, 5379–5388. [[CrossRef](#)]
38. Shcherbakov, V.; Denisov, S.A.; Mostafavi, M. On the Primary Water Radicals' Production in the Presence of Gold Nanoparticles: Electron Pulse Radiolysis Study. *Nanomaterials* **2020**, *10*, 2478. [[CrossRef](#)]
39. Howard, D.; Sebastian, S.; Le, Q.V.-C.; Thierry, B.; Kempson, I. Chemical Mechanisms of Nanoparticle Radiosensitization and Radioprotection: A Review of Structure-Function Relationships Influencing Reactive Oxygen Species. *Int. J. Mol. Sci.* **2020**, *21*, 579. [[CrossRef](#)]
40. Minai, L.; Yeheskely-Hayon, D.; Yelin, D. High levels of reactive oxygen species in gold nanoparticle-targeted cancer cells following femtosecond pulse irradiation. *Sci. Rep.* **2013**, *3*, srep02146. [[CrossRef](#)]
41. Jawaid, P.; Rehman, M.U.; Zhao, Q.-L.; Misawa, M.; Ishikawa, K.; Hori, M.; Shimizu, T.; Saitoh, J.-I.; Noguchi, K.; Kondo, T. Small size gold nanoparticles enhance apoptosis-induced by cold atmospheric plasma via depletion of intracellular GSH and modification of oxidative stress. *Cell Death Discov.* **2020**, *6*, 83. [[CrossRef](#)]
42. Shcherbakov, V.; Denisov, S.A.; Mostafavi, M. Selective Oxidation of Transient Organic Radicals in the Presence of Gold Nanoparticles. *Nanomaterials* **2021**, *11*, 727. [[CrossRef](#)]
43. Singh, P.; Pandit, S.; Mokkapatil, V.; Garg, A.; Ravikumar, V.; Mijakovic, I. Gold Nanoparticles in Diagnostics and Therapeutics for Human Cancer. *Int. J. Mol. Sci.* **2018**, *19*, 1979. [[CrossRef](#)] [[PubMed](#)]
44. Luo, D.; Wang, X.; Zeng, S.; Ramamurthy, G.; Burda, C.; Basilion, J.P. Prostate-specific membrane antigen targeted gold nanoparticles for prostate cancer radiotherapy: Does size matter for targeted particles? *Chem. Sci.* **2019**, *10*, 8119–8128. [[CrossRef](#)] [[PubMed](#)]
45. Farahani, S.; Alam, N.R.; Haghgo, S.; Khoobi, M.; Geraily, G.H.; Gorji, E. Dosimetry and radioenhancement comparison of gold nanoparticles in kilovoltage and megavoltage radiotherapy using MAGAT polymer gel dosimeter. *J. Biomed. Phys. Eng.* **2019**, *9*, 199. [[CrossRef](#)]
46. Konefał, A.; Lniak, W.; Rostocka, J.; Orlef, A.; Sokół, M.; Kasperczyk, J.; Jarzabek, P.; Wrońska, A.; Rusiecka, K. Influence of a shape of gold nanoparticles on the dose enhancement in the wide range of gold mass concentration for high-energy X-ray beams from a medical linac. *Rep. Pract. Oncol. Radiother.* **2020**, *25*, 579–585. [[CrossRef](#)] [[PubMed](#)]
47. Tudda, A.; Donzelli, E.; Nicolini, G.; Semperboni, S.; Bossi, M.; Cavaletti, G.; Castriconi, R.; Mangili, P.; del Vecchio, A.; Sarno, A.; et al. Breast radiotherapy with kilovoltage photons and gold nanoparticles as radiosensitizer: An in vitro study. *Med. Phys.* **2022**, *49*, 568–578. [[CrossRef](#)]
48. Yogo, K.; Misawa, M.; Shimizu, H.; Kitagawa, T.; Hirayama, R.; Ishiyama, H.; Yasuda, H.; Kametaka, S.; Takami, S. Radiosensitization Effect of Gold Nanoparticles on Plasmid DNA Damage Induced by Therapeutic MV X-rays. *Nanomaterials* **2022**, *12*, 771. [[CrossRef](#)]
49. Abdollahi, B.B.; Malekzadeh, R.; Azar, F.P.; Salehnia, F.; Naseri, A.R.; Ghorbani, M.; Hamishehkar, H.; Farajollahi, A.R. Main Approaches to Enhance Radiosensitization in Cancer Cells by Nanoparticles: A Systematic Review. *Adv. Pharm. Bull.* **2020**, *11*, 212–223. [[CrossRef](#)]
50. McMahan, S.J.; Hyland, W.B.; Muir, M.F.; Coulter, J.A.; Jain, S.; Butterworth, K.T.; Schettino, G.; Dickson, G.R.; Hounsell, A.R.; O'Sullivan, J.M.; et al. Biological consequences of nanoscale energy deposition near irradiated heavy atom nanoparticles. *Sci. Rep.* **2011**, *1*, 18. [[CrossRef](#)]
51. Bhattacharyya, S.; Kudgus, R.A.; Bhattacharya, R.; Mukherjee, P. Inorganic Nanoparticles in Cancer Therapy. *Pharm. Res.* **2011**, *28*, 237–259. [[CrossRef](#)]
52. Rahman, W.N.; Bishara, N.; Ackerly, T.; He, C.F.; Jackson, P.; Wong, C.; Davidson, R.; Geso, M. Enhancement of radiation effects by gold nanoparticles for superficial radiation therapy. *Nanomed. Nanotechnol. Biol. Med.* **2009**, *5*, 136–142. [[CrossRef](#)]

53. Guerra, D.B.; Oliveira, E.M.N.; Sonntag, A.R.; Sbaraine, P.; Fay, A.P.; Morrone, F.B.; Papaléo, R.M. Intercomparison of radiosensitization induced by gold and iron oxide nanoparticles in human glioblastoma cells irradiated by 6 MV photons. *Sci. Rep.* **2022**, *12*, 9602. [CrossRef]
54. Gregersen, E. Gadolinium chemical element. In *Britannica*; The Editors of Encyclopaedia, Ed.; Encyclopedia Britannica: Chicago, IL, USA, 2022.
55. American Elements. Gadolinium Nanoparticles. Available online: <https://www.americanelements.com/gadolinium-nanoparticles-7440-54-2> (accessed on 15 April 2023).
56. Cao, M.; Wang, P.; Kou, Y.; Wang, J.; Liu, J.; Li, Y.-H.; Li, J.; Wang, L.; Chen, C. Gadolinium(III)-Chelated Silica Nanospheres Integrating Chemotherapy and Photothermal Therapy for Cancer Treatment and Magnetic Resonance Imaging. *ACS Appl. Mater. Interfaces* **2015**, *7*, 25014–25023. [CrossRef]
57. Ahmad, M.Y.; Ahmad, W.; Yue, H.; Ho, S.L.; Park, J.A.; Jung, K.-H.; Cha, H.; Marasini, S.; Ghazanfari, A.; Liu, S.; et al. In Vivo Positive Magnetic Resonance Imaging Applications of Poly(methyl vinyl ether-alt-maleic acid)-coated Ultra-small Paramagnetic Gadolinium Oxide Nanoparticles. *Molecules* **2020**, *25*, 1159. [CrossRef]
58. Mortezaadeh, T.; Gholibegloo, E.; Alam, N.R.; Dehghani, S.; Haghgoo, S.; Ghanaati, H.; Khoobi, M. Gadolinium (III) oxide nanoparticles coated with folic acid-functionalized poly( $\beta$ -cyclodextrin-co-pentetic acid) as a biocompatible targeted nano-contrast agent for cancer diagnostic: In vitro and in vivo studies. *Magn. Reson. Mater. Phys. Biol. Med.* **2019**, *32*, 487–500. [CrossRef]
59. Toth, E.; Helm, L.; Merbach, A. Relaxivity of gadolinium (III) complexes: Theory and mechanism. In *The Chemistry of Contrast Agents in Medical Magnetic Resonance Imaging*; Wiley: Hoboken, NJ, USA, 2013; pp. 25–81.
60. Yue, H.; Park, J.Y.; Chang, Y.; Lee, G.H. Ultrasmall Europium, Gadolinium, and Dysprosium Oxide Nanoparticles: Polyol Synthesis, Properties, and Biomedical Imaging Applications. *Mini-Reviews Med. Chem.* **2020**, *20*, 1767–1780. [CrossRef]
61. Kochebina, O.; Halty, A.; Taleb, J.; Kryza, D.; Janier, M.; Sadr, A.B.; Baudier, T.; Rit, S.; Sarrut, D. In vivo gadolinium nanoparticle quantification with SPECT/CT. *EJNMMI Phys.* **2019**, *6*, 9. [CrossRef]
62. Cho, M.; Sethi, R.; Narayanan, J.S.A.; Lee, S.S.; Benoit, D.N.; Taheri, N.; Decuzzi, P.; Colvin, V.L. Gadolinium oxide nanoplates with high longitudinal relaxivity for magnetic resonance imaging. *Nanoscale* **2014**, *6*, 13637–13645. [CrossRef]
63. Dai, Y.; Wu, C.; Wang, S.; Li, Q.; Zhang, M.; Li, J.; Xu, K. Comparative study on in vivo behavior of PEGylated gadolinium oxide nanoparticles and Magnevist as MRI contrast agent. *Nanomed. Nanotechnol. Biol. Med.* **2018**, *14*, 547–555. [CrossRef]
64. Catanzaro, V.; Digilio, G.; Capuana, F.; Padovan, S.; Cutrin, J.C.; Carniato, F.; Porta, S.; Grange, C.; Filipović, N.; Stevanović, M. Gadolinium-Labelled Cell Scaffolds to Follow-up Cell Transplantation by Magnetic Resonance Imaging. *J. Funct. Biomater.* **2019**, *10*, 28. [CrossRef]
65. Lu, R.; Zhang, Y.; Tao, H.; Zhou, L.; Li, H.; Chen, T.; Zhang, P.; Lu, Y.; Chen, S. Gadolinium-hyaluronic acid nanoparticles as an efficient and safe magnetic resonance imaging contrast agent for articular cartilage injury detection. *Bioact. Mater.* **2020**, *5*, 758–767. [CrossRef]
66. Schulte-Altendorfer, G.; Gebhard, M.; Wohlgemuth, W.; Fischer, W.; Zentner, J.; Wegener, R.; Balzer, T.; Bohndorf, K. MR arthrography: Pharmacology, efficacy and safety in clinical trials. *Skelet. Radiol.* **2003**, *32*, 1–12. [CrossRef] [PubMed]
67. Wu, B.; Lu, S.-T.; Yu, H.; Liao, R.-F.; Li, H.; Lucie Zafitatisimo, B.V.; Li, Y.-S.; Zhang, Y.; Zhu, X.-L.; Liu, H.-G.; et al. Gadolinium-chelate functionalized bismuth nanotheranostic agent for in vivo MRI/CT/PAI imaging-guided photothermal cancer therapy. *Biomaterials* **2018**, *159*, 37–47. [CrossRef] [PubMed]
68. Aime, S.; Caravan, P. Biodistribution of gadolinium-based contrast agents, including gadolinium deposition. *J. Magn. Reson. Imaging Off. J. Int. Soc. Magn. Reson. Med.* **2009**, *30*, 1259–1267. [CrossRef] [PubMed]
69. Wu, B.; Li, X.-Q.; Huang, T.; Lu, S.-T.; Wan, B.; Liao, R.-F.; Li, Y.-S.; Baidya, A.; Long, Q.-Y.; Xu, H.-B. MRI-guided tumor chemo-photodynamic therapy with Gd/Pt bifunctionalized porphyrin. *Biomater. Sci.* **2017**, *5*, 1746–1750. [CrossRef] [PubMed]
70. Jahanbin, T.; Sauriat-Dorizon, H.; Spearman, P.; Benderbous, S.; Korri-Youssoufi, H. Development of Gd(III) porphyrin-conjugated chitosan nanoparticles as contrast agents for magnetic resonance imaging. *Mater. Sci. Eng. C* **2015**, *52*, 325–332. [CrossRef]
71. Lovell, J.F.; Jin, C.S.; Huynh, E.; Jin, H.; Kim, C.; Rubinstein, J.L.; Chan, W.C.W.; Cao, W.; Wang, L.V.; Zheng, G. Porphysome nanovesicles generated by porphyrin bilayers for use as multimodal biophotonic contrast agents. *Nat. Mater.* **2011**, *10*, 324–332. [CrossRef]
72. Tamiaki, H.; Unno, S.; Takeuchi, E.; Tameshige, N.; Shinoda, S.; Tsukube, H. Induced circular dichroism by complexation of gadolinium(III) porphyrinates with chiral amino acids and dipeptides: Effects of axial  $\beta$ -diketonate ligands on chirality sensing and recognition. *Tetrahedron* **2003**, *59*, 10477–10483. [CrossRef]
73. Heitmann, G.; Schütt, C.; Gröbner, J.; Huber, L.; Herges, R. Azoimidazole functionalized Ni-porphyrins for molecular spin switching and light responsive MRI contrast agents. *Dalton Trans.* **2016**, *45*, 11407–11412. [CrossRef]
74. Winter, M.B.; Klemm, P.J.; Phillips-Piro, C.M.; Raymond, K.N.; Marletta, M.A. Porphyrin-Substituted H-NOX Proteins as High-Relaxivity MRI Contrast Agents. *Inorg. Chem.* **2013**, *52*, 2277–2279. [CrossRef]
75. Zhou, Y.; Liang, X.; Dai, Z. Porphyrin-loaded nanoparticles for cancer theranostics. *Nanoscale* **2016**, *8*, 12394–12405. [CrossRef]
76. Liu, F.; Ma, Y.; Xu, L.; Liu, L.; Zhang, W. Redox-responsive supramolecular amphiphiles constructed via host–guest interactions for photodynamic therapy. *Biomater. Sci.* **2015**, *3*, 1218–1227. [CrossRef]
77. Malina, L.; Tomankova, K.B.; Malohlava, J.; Jiravova, J.; Manisova, B.; Zapletalova, J.; Kolarova, H. The in vitro cytotoxicity of metal-complexes of porphyrin sensitizer intended for photodynamic therapy. *Toxicol. In Vitro* **2016**, *34*, 246–256. [CrossRef]

78. Li, B.; Sun, L.; Li, T.; Zhang, Y.; Niu, X.; Xie, M.; You, Z. Ultra-small gold nanoparticles self-assembled by gadolinium ions for enhanced photothermal/photodynamic liver cancer therapy. *J. Mater. Chem. B* **2021**, *9*, 1138–1150. [[CrossRef](#)]
79. Coughlin, A.J.; Ananta, J.S.; Deng, N.; Larina, I.V.; Decuzzi, P.; West, J.L. Gadolinium-Conjugated Gold Nanoshells for Multimodal Diagnostic Imaging and Photothermal Cancer Therapy. *Small* **2014**, *10*, 556–565. [[CrossRef](#)]
80. Verry, C.; Sancey, L.; Dufort, S.; Le Duc, G.; Mendoza, C.; Lux, F.; Grand, S.; Arnaud, J.; Quesada, J.L.; Villa, J.; et al. Treatment of multiple brain metastases using gadolinium nanoparticles and radiotherapy: NANO-RAD, a phase I study protocol. *BMJ Open* **2019**, *9*, e023591. [[CrossRef](#)]
81. Verry, C.; Dufort, S.; Villa, J.; Gavard, M.; Iriart, C.; Grand, S.; Charles, J.; Chovelon, B.; Cracowski, J.-L.; Quesada, J.-L.; et al. Theranostic AGuIX nanoparticles as radiosensitizer: A phase I, dose-escalation study in patients with multiple brain metastases (NANO-RAD trial). *Radiother. Oncol.* **2021**, *160*, 159–165. [[CrossRef](#)]
82. Salt, C.; Lennox, A.J.; Takagaki, M.; Maguire, J.A.; Hosmane, N.S. Boron and gadolinium neutron capture therapy. *Russ. Chem. Bull.* **2004**, *53*, 1871–1888. [[CrossRef](#)]
83. Brugger, R.M.; Shih, J.A. Evaluation of gadolinium-157 as a neutron capture therapy agent. *Strahlenther. Onkol.* **1989**, *165*, 153–156.
84. Akine, Y.; Tokita, N.; Tokuyue, K.; Satoh, M.; Churei, H.; Le Pechoux, C.; Kobayashi, T.; Kanda, K. Suppression of Rabbit VX-2 Subcutaneous Tumor Growth by Gadolinium Neutron Capture Therapy. *Jpn. J. Cancer Res.* **1993**, *84*, 841–843. [[CrossRef](#)]
85. Deagostino, A.; Protti, N.; Alberti, D.; Boggio, P.; Bortolussi, S.; Altieri, S.; Crich, S.G. Insights into the use of gadolinium and gadolinium/boron-based agents in imaging-guided neutron capture therapy applications. *Futur. Med. Chem.* **2016**, *8*, 899–917. [[CrossRef](#)]
86. Perry, H.L.; Botnar, R.M.; Wilton-Ely, J.D.E.T. Gold nanomaterials functionalised with gadolinium chelates and their application in multimodal imaging and therapy. *Chem. Commun.* **2020**, *56*, 4037–4046. [[CrossRef](#)] [[PubMed](#)]
87. Lancelot, E.; Desché, P. Gadolinium retention as a safety signal: Experience of a manufacturer. *Investig. Radiol.* **2020**, *55*, 20. [[CrossRef](#)] [[PubMed](#)]
88. Yaseen, M.; Humayun, M.; Khan, A.; Usman, M.; Ullah, H.; Tahir, A.A.; Ullah, H. Preparation, Functionalization, Modification, and Applications of Nanostructured Gold: A Critical Review. *Energies* **2021**, *14*, 1278. [[CrossRef](#)]
89. Sharma, J.; Chhabra, R.; Yan, H.; Liu, Y. A facile in situ generation of dithiocarbamate ligands for stable gold nanoparticle-oligonucleotide conjugates. *Chem. Commun.* **2008**, *18*, 2140–2142. [[CrossRef](#)] [[PubMed](#)]
90. Perry, H.L.; Yoon, I.-C.; Chabloz, N.G.; Molisso, S.; Stasiuk, G.J.; Botnar, R.; Wilton-Ely, J.D.E.T. Metallostar Assemblies Based on Dithiocarbamates for Use as MRI Contrast Agents. *Inorg. Chem.* **2020**, *59*, 10813–10823. [[CrossRef](#)]
91. Lohrke, J.; Frenzel, T.; Endrikat, J.; Alves, F.C.; Grist, T.M.; Law, M.; Lee, J.M.; Leiner, T.; Li, K.-C.; Nikolaou, K.; et al. 25 Years of Contrast-Enhanced MRI: Developments, Current Challenges and Future Perspectives. *Adv. Ther.* **2016**, *33*, 1–28. [[CrossRef](#)]
92. Wahsner, J.; Gale, E.M.; Rodríguez-Rodríguez, A.; Caravan, P. Chemistry of MRI Contrast Agents: Current Challenges and New Frontiers. *Chem. Rev.* **2018**, *119*, 957–1057. [[CrossRef](#)]
93. Holbrook, R.J.; Rammohan, N.; Rotz, M.W.; MacRenaris, K.W.; Preslar, A.T.; Meade, T.J. Gd(III)-Dithiolane Gold Nanoparticles for T<sub>1</sub>-Weighted Magnetic Resonance Imaging of the Pancreas. *Nano Lett.* **2016**, *16*, 3202–3209. [[CrossRef](#)]
94. Fatehbasharad, P.; Stefania, R.; Carrera, C.; Hawala, I.; Castelli, D.D.; Baroni, S.; Colombo, M.; Prosperi, D.; Aime, S. Relaxometric studies of gd-chelate conjugated on the surface of differently shaped gold nanoparticles. *Nanomaterials* **2020**, *10*, 1115. [[CrossRef](#)]
95. Chabloz, N.G.; Wenzel, M.N.; Perry, H.L.; Yoon, I.; Molisso, S.; Stasiuk, G.J.; Elson, D.; Cass, A.E.G.; Wilton-Ely, J.D.E.T. Polyfunctionalised Nanoparticles Bearing Robust Gadolinium Surface Units for High Relaxivity Performance in MRI. *Chem.—A Eur. J.* **2019**, *25*, 10895–10906. [[CrossRef](#)]
96. Aouidat, F.; Boumati, S.; Khan, M.; Tielens, F.; Doan, B.T.; Spadavecchia, J. Design and synthesis of gold-gadolinium-core-shell nanoparticles as contrast agent: A smart way to future nanomaterials for nanomedicine applications. *Int. J. Nanomed.* **2019**, *14*, 9309. [[CrossRef](#)]
97. Samadian, H.; Hosseini-Nami, S.; Kamrava, S.K.; Ghaznavi, H.; Shakeri-Zadeh, A. Folate-conjugated gold nanoparticle as a new nanoplatform for targeted cancer therapy. *J. Cancer Res. Clin. Oncol.* **2016**, *142*, 2217–2229. [[CrossRef](#)]
98. Lee, D.-E.; Koo, H.; Sun, I.-C.; Ryu, J.H.; Kim, K.; Kwon, I.C. Multifunctional nanoparticles for multimodal imaging and theragnosis. *Chem. Soc. Rev.* **2012**, *41*, 2656–2672. [[CrossRef](#)]
99. Qin, H.; Zhou, T.; Yang, S.; Chen, Q.; Xing, D. Gadolinium(III)-gold nanorods for MRI and photoacoustic imaging dual-modality detection of macrophages in atherosclerotic inflammation. *Nanomedicine* **2013**, *8*, 1611–1624. [[CrossRef](#)]
100. Cherukula, K.; Manickavasagam Lekshmi, K.; Uthaman, S.; Cho, K.; Cho, C.-S.; Park, I.-K. Multifunctional Inorganic Nanoparticles: Recent Progress in Thermal Therapy and Imaging. *Nanomaterials* **2016**, *6*, 76. [[CrossRef](#)]
101. Degrauwe, N.; Hocquelet, A.; Digkila, A.; Schaefer, N.; Denys, A.; Duran, R. Theranostics in Interventional Oncology: Versatile Carriers for Diagnosis and Targeted Image-Guided Minimally Invasive Procedures. *Front. Pharmacol.* **2019**, *10*, 450. [[CrossRef](#)]
102. Hou, W.; Xia, F.; Alfranca, G.; Yan, H.; Zhi, X.; Liu, Y.; Peng, C.; Zhang, C.; de la Fuente, J.M.; Cui, D. Nanoparticles for multimodality cancer diagnosis: Simple protocol for self-assembly of gold nanoclusters mediated by gadolinium ions. *Biomaterials* **2017**, *120*, 103–114. [[CrossRef](#)]
103. Zhou, B.; Xiong, Z.; Wang, P.; Peng, C.; Shen, M.; Mignani, S.; Majoral, J.-P.; Shi, X. Targeted tumor dual mode CT/MR imaging using multifunctional polyethylenimine-entrapped gold nanoparticles loaded with gadolinium. *Drug Deliv.* **2018**, *25*, 178–186. [[CrossRef](#)]

104. Zhang, C.; Xu, Z.; Di, H.; Zeng, E.; Jiang, Y.; Liu, D. Gadolinium-doped Au@prussian blue nanoparticles as MR/SERS bimodal agents for dendritic cell activating and tracking. *Theranostics* **2020**, *10*, 6061–6071. [[CrossRef](#)]
105. Pitchaimani, A.; Nguyen TD, T.; Maurmann, L.; Key, J.; Bossmann, S.H.; Aryal, S. Gd<sup>3+</sup> tethered gold nanorods for combined magnetic resonance imaging and photo-thermal therapy. *J. Biomed. Nanotechnol.* **2017**, *13*, 417–426. [[CrossRef](#)]
106. Gao, Y.; Li, Y.; Chen, J.; Zhu, S.; Liu, X.; Zhou, L.; Shi, P.; Niu, D.; Gu, J.; Shi, J. Multifunctional gold nanostar-based nanocomposite: Synthesis and application for noninvasive MR-SERS imaging-guided photothermal ablation. *Biomaterials* **2015**, *60*, 31–41. [[CrossRef](#)] [[PubMed](#)]
107. Cheng, Y.; Meyers, J.D.; Broome, A.-M.; Kenney, M.E.; Basilion, J.P.; Burda, C. Deep Penetration of a PDT Drug into Tumors by Noncovalent Drug-Gold Nanoparticle Conjugates. *J. Am. Chem. Soc.* **2011**, *133*, 2583–2591. [[CrossRef](#)] [[PubMed](#)]
108. Liu, J.; Wang, D.; Wang, G. Magnetic-gold theranostic nanoagent used for targeting quad modalities T 1 & T 2-MRI/CT/PA imaging and photothermal therapy of tumours. *RSC Adv.* **2021**, *11*, 18440–18447. [[PubMed](#)]
109. Caravan, P.; Esteban-Gómez, D.; Rodríguez-Rodríguez, A.; Platas-Iglesias, C. Water exchange in lanthanide complexes for MRI applications. Lessons learned over the last 25 years. *Dalton Trans.* **2019**, *48*, 11161–11180. [[CrossRef](#)] [[PubMed](#)]
110. Khan, M.; Boumati, S.; Arib, C.; Diallo, A.T.; Djaker, N.; Doan, B.-T.; Spadavecchia, J. Doxorubicin (DOX) Gadolinium–Gold-Complex: A New Way to Tune Hybrid Nanorods as Theranostic Agent. *Int. J. Nanomed.* **2021**, *16*, 2219–2236. [[CrossRef](#)]
111. Usman, M.S.; Hussein, M.Z.; Fakurazi, S.; Masarudin, M.J.; Saad, F.F.A. Gadolinium-doped gallic acid-zinc/aluminium-layered double hydroxide/gold theranostic nanoparticles for a bimodal magnetic resonance imaging and drug delivery system. *Nanomaterials* **2017**, *7*, 244. [[CrossRef](#)]
112. Usman, M.S.; Hussein, M.Z.; Fakurazi, S.; Masarudin, M.J.; Saad, F.F.A. A bimodal theranostic nanodelivery system based on [graphene oxide-chlorogenic acid-gadolinium/gold] nanoparticles. *PLoS ONE* **2018**, *13*, e0200760. [[CrossRef](#)]
113. Han, L.; Xia, J.-M.; Hai, X.; Shu, Y.; Chen, X.-W.; Wang, J.-H. Protein-Stabilized Gadolinium Oxide-Gold Nanoclusters Hybrid for Multimodal Imaging and Drug Delivery. *ACS Appl. Mater. Interfaces* **2017**, *9*, 6941–6949. [[CrossRef](#)]
114. Miladi, I.; Alric, C.; Dufort, S.; Mowat, P.; Dutour, A.; Mandon, C.; Laurent, G.; Bräuer-Krisch, E.; Herath, N.; Coll, J.-L.; et al. The In Vivo Radiosensitizing Effect of Gold Nanoparticles Based MRI Contrast Agents. *Small* **2014**, *10*, 1116–1124. [[CrossRef](#)]
115. Durand, M.; Lelievre, E.; Chateau, A.; Berquand, A.; Laurent, G.; Carl, P.; Roux, S.; Chazee, L.; Bazzi, R.; Eghiaian, F.; et al. The detrimental invasiveness of glioma cells controlled by gadolinium chelate-coated gold nanoparticles. *Nanoscale* **2021**, *13*, 9236–9251. [[CrossRef](#)]
116. Debouttière, P.-J.; Roux, S.; Vocanson, F.; Billotey, C.; Beuf, O.; Favre-Reguillon, A.; Lin, Y.; Pellet-Rostaing, S.; Lamartine, R.; Perriat, P.; et al. Design of Gold Nanoparticles for Magnetic Resonance Imaging. *Adv. Funct. Mater.* **2006**, *16*, 2330–2339. [[CrossRef](#)]
117. Tomić, S.; Đokić, J.; Vasilijić, S.; Ogrinc, N.; Rudolf, R.; Pelicon, P.; Vučević, D.; Milosavljević, P.; Janković, S.; Anžel, I.; et al. Size-Dependent Effects of Gold Nanoparticles Uptake on Maturation and Antitumor Functions of Human Dendritic Cells In Vitro. *PLoS ONE* **2014**, *9*, e96584. [[CrossRef](#)]
118. Qiu, T.A.; Bozich, J.S.; Lohse, S.E.; Vartanian, A.M.; Jacob, L.M.; Meyer, B.M.; Gunsolus, I.L.; Niemuth, N.J.; Murphy, C.J.; Haynes, C.L.; et al. Gene expression as an indicator of the molecular response and toxicity in the bacterium *Shewanella oneidensis* and the water flea *Daphnia magna* exposed to functionalized gold nanoparticles. *Environ. Sci. Nano* **2015**, *2*, 615–629. [[CrossRef](#)]
119. Hühn, D.; Kantner, K.; Geidel, C.; Brandholt, S.; De Cock, I.; Soenen, S.J.H.; Rivera\_Gil, P.; Montenegro, J.-M.; Braeckmans, K.; Müllen, K.; et al. Polymer-Coated Nanoparticles Interacting with Proteins and Cells: Focusing on the Sign of the Net Charge. *ACS Nano* **2013**, *7*, 3253–3263. [[CrossRef](#)]
120. Deng, J.; Yao, M.; Gao, C. Cytotoxicity of gold nanoparticles with different structures and surface-anchored chiral polymers. *Acta Biomater.* **2017**, *53*, 610–618. [[CrossRef](#)]
121. Hou, H.; Chen, L.; He, H.; Chen, L.; Zhao, Z.; Jin, Y. Fine-tuning the LSPR response of gold nanorod–polyaniline core–shell nanoparticles with high photothermal efficiency for cancer cell ablation. *J. Mater. Chem. B* **2015**, *3*, 5189–5196. [[CrossRef](#)]
122. Thierry, B.; Ng, J.; Krieg, T.; Griesser, H.J. A robust procedure for the functionalization of gold nanorods and noble metal nanoparticles. *Chem. Commun.* **2009**, *13*, 1724–1726. [[CrossRef](#)]

**Disclaimer/Publisher’s Note:** The statements, opinions and data contained in all publications are solely those of the individual author(s) and contributor(s) and not of MDPI and/or the editor(s). MDPI and/or the editor(s) disclaim responsibility for any injury to people or property resulting from any ideas, methods, instructions or products referred to in the content.